THE EFFECT OF SOLIDS CONCENTRATION AND PARTICLE PROPERTIES ON CLOUD HEIGHT IN TALL STIRRED TANKS

A THESIS SUBMITTED TO
THE GRADUATE SCHOOL OF NATURAL AND APPLIED SCIENCES
OF
MIDDLE EAST TECHNICAL UNIVERSITY

BY

EZGİ ALTINTAŞ

IN PARTIAL FULFILLMENT OF THE REQUIREMENTS
FOR
THE DEGREE OF MASTER OF SCIENCE
IN
CHEMICAL ENGINEERING

JUNE 2021

Approval of the thesis:

THE EFFECT OF SOLIDS CONCENTRATION AND PARTICLE PROPERTIES ON CLOUD HEIGHT IN TALL STIRRED TANKS

submitted by **EZGİ ALTINTAŞ** in partial fulfillment of the requirements for the degree of **Master of Science** i**n Chemical Engineering, Middle East Technical University** by,

Prof. Dr. Halil Kalıpçılar
Dean, Graduate School of **Natural and Applied Sciences** _____

Prof. Dr. Pınar Çalık
Head of the Department, **Chemical Engineering** _____

Assoc. Prof. İnci Ayrancı Tansık
Supervisor, **Chemical Engineering, METU** _____

Examining Committee Members:

Prof. Dr. Yusuf Uludağ
Chemical Engineering, METU _____

Assoc. Prof. İnci Ayrancı Tansık
Chemical Engineering, METU _____

Prof. Dr. Görkem Külah
Chemical Engineering, METU _____

Asst. Prof. Gökhan Çelik
Chemical Engineering, METU _____

Assoc. Prof. Suna Ertunç
Chemical Engineering, Ankara University _____

Date: 04.06.2021

I hereby declare that all information in this document has been obtained and presented in accordance with academic rules and ethical conduct. I also declare that, as required by these rules and conduct, I have fully cited and referenced all material and results that are not original to this work.

Name Last name : Ezgi Altıntaş

Signature :

ABSTRACT

THE EFFECT OF SOLIDS CONCENTRATION AND PARTICLE PROPERTIES ON CLOUD HEIGHT IN TALL STIRRED TANKS

Altıntaş, Ezgi
Master of Science, Chemical Engineering
Supervisor : Assoc. Prof. İnci Ayrancı Tansık

June 2021, 95 pages

Solid-liquid mixing is one of the most commonly used unit operations in industries such as petrochemicals, polymer processing, biotechnology, pharmaceuticals, and mineral processing. There are two focuses in solid-liquid mixing operations: solids suspension and solids distribution. The key design parameter for solids suspension is N_{js}. In most solids suspensions, the main objective is to provide maximum contact between solid and liquid phases with minimum power consumption, and this can be achieved by setting the impeller speed (N) to N_{js}. The key design parameter for solids distribution is cloud height. At high solids concentrations (X_V) the solids can reach a level beyond which the concentration of the solids dramatically drops. This level appears like an interface between solid-rich and liquid-rich parts of the tank. The height of this interface is known as cloud height.

Due to the fluctuating nature of cloud height its measurement is not straightforward. Despite this, there is no clearly defined measurement point of cloud height in literature. Besides, the current definition of cloud height does not involve any limitations on X_V and N, which are two parameters that significantly affect hydrodynamics in a stirred tank, and thus the cloud height. To obtain meaningful

cloud height data, a measurement point of cloud height should be determined; likewise, limitations on X_V and N should be identified.

This study aims to propose a clarified definition of cloud height that takes X_V and N into account, to investigate the effects of X_V and particle properties on cloud height and propose a correlation to predict cloud height. A flat-bottomed tank in which liquid level was equal to 1.5 tank diameter (H=1.5T) was used with four equally spaced baffles. A 45° pitched blade turbine (PBT) was used as an impeller. Six different particles were used in the experiments.

According to observations, in the tank, efficient solid-liquid mixing takes place until the maximum point that solids can reach in the axial direction. Beyond this, only rare bursts of a small portion of solids were observed. The measurement point of cloud height, therefore, was determined as the maximum level that solids can reach. This corresponds to the front of the baffle for the configuration tested. The limitations on X_V and N for the measurement of cloud height were identified using this measurement point. According to findings, to observe a meaningful cloud height, X_V should be at and above 2 vol% and N should be at and above $0.32N_{js}$. For a H=1.5T tank, a meaningful cloud height can be observed until N is equal to $1.45N_{js}$, at which all solids are distributed throughout the tank and no interface can be observed. It was also found that beyond 9 vol% cloud height remains constant.

After limitations of X_V and N on cloud height were determined, the effect of X_V, particle properties and off-bottom clearance (C/T) on cloud height was investigated. The results showed that cloud height is a strong function of X_V and C/T; but not a strong function of particle properties. Based on the findings, a purely empirical model that predicts cloud height as a function of X_V, particle properties and C/T was proposed.

Keywords: Solids Suspensions, Cloud Height, High Solids Concentration, Tall Tanks

ÖZ

UZUN KARIŞTIRMA TANKLARINDA KATI KONSANTRASYONUNUN VE PARTİKÜL ÖZELLİKLERİNİN BULUT YÜKSEKLİĞİNE ETKİSİ

Altıntaş, Ezgi
Yüksek Lisans, Kimya Mühendisliği
Tez Yöneticisi: Doç. Dr. İnci Ayrancı Tansık

Haziran 2021, 95 sayfa

Katı-sıvı karıştırma prosesi petrokimya, polimer işleme, biyoteknoloji, ilaç ve mineral işleme gibi sektörlerde kullanılan en yaygın temel işlemlerden biridir. Katı-sıvı karıştırmada iki odak noktası vardır: katı süspansiyonu ve katı dağılımı. Katı süspansiyonları için anahtar tasarım parametresi N_{js}'dir. Çoğu katı süspansiyonda temel amaç, minimum güç tüketimi ile katı ve sıvı fazlar arasında maksimum temas sağlamaktır ve bu, karıştırıcı hızı (N) değerinin N_{js}'e ayarlanmasıyla sağlanabilir. Katı dağılımı için anahtar tasarım parametresi bulut yüksekliği'dir. Yüksek katı konsantrasyonu (X_V) değerlerinde katılar, ötesinde konsantrasyonun önemli ölçüde düştüğü bir seviyeye kadar ulaşabilirler. Bu seviye, tankın katı bakımından zengin ve sıvı bakımından zengin kısımları arasındaki bir arayüz gibi görünmektedir. Bu arayüzün yüksekliği bulut yüksekliği olarak bilinmektedir.

Bulut yüksekliği'nin dalgalı doğası nedeniyle ölçümü kolay değildir. Buna rağmen literatürde bulut yüksekliği'nin belirli bir ölçüm noktası yoktur. Ayrıca, mevcut tanım, bir karıştırma tankı içindeki hidrodinamiği ve dolayısıyla bulut yüksekliği'ni önemli ölçüde etkileyen X_V ve N üzerine hiçbir sınırlama içermez. Anlamlı bulut

yüksekliği verileri elde etmek için bir ölçüm noktası belirlenmelidir. Benzer şekilde, X_V ve N ile ilgili sınırlamalar tanımlanmalıdır.

Bu çalışma, X_V ve N parametrelerini hesaba katan net bir bulut yüksekliği tanımı önermeyi, X_V ve N'in bulut yüksekliği üzerindeki etkilerini incelemeyi ve bulut yüksekliği'ni hesaplamak için bir deneysel eşitlik önermeyi amaçlamaktadır. Bu çalışmada, su seviyesinin tank çapının 1.5 katına eşit olduğu düz tabanlı bir tank, eşit aralıklarla yerleştirilmiş dört engel ile kullanılmıştır. Karıştırıcı olarak 45° eğimli bıçaklı karıştırıcı (PBT) kullanılmıştır. Deneylerde altı farklı tanecik kullanılmıştır.

Gözlemlere göre, verimli bir katı-sıvı karıştırma, tank içinde katıların ulaşabileceği en yüksek noktaya kadar sağlanabilir. Bu noktanın ötesinde, katıların sadece küçük bir kısmının nadir gerçekleşen sıçramaları gözlemlenmiştir. Böylelikle, bulut yüksekliği'nin ölçüm noktası, katıların ulaşabileceği en yüksek nokta olarak belirlenmiştir. Bu nokta, kullanılan deneysel düzen için engelin ön kısmına denk gelmektedir. Belirlenen ölçüm noktası kullanılarak X_V ve N sınırları tespit edilmiştir. Bulgulara göre, anlamlı bir bulut yüksekliği gözlemlemek için X_V hacimce %2 ve üzerinde; N ise $0.32N_{js}$ ve üzerinde olmalıdır. H=1.5T olan bir tankta, anlamlı bir bulut yüksekliği $N=1.45N_{js}$ olana kadar gözlemlenebilir çünkü bu karıştırıcı hızında tüm katılar tank boyunca dağıtılır ve artık bir arayüz gözlemlenemez. Ek olarak, X_V hacimce %9'un üzerindeyken bulut yüksekliği'nin değişmediği görülmüştür. X_V ve N sınırları belirlendikten sonra, X_V, tanecik özellikleri ve karıştırıcının tank tabanından yüksekliğinin (C/T) bulut yüksekliği üzerindeki etkileri araştırılmıştır. Bulgular, bulut yüksekliği'nin, X_V ve C/T'nin güçlü bir fonksiyonu olduğunu; ancak tanecik özelliklerinin güçlü bir fonksiyonu olmadığını göstermiştir. Bulgulara dayanarak, bulut yüksekliği'ni X_V, tanecik özellikleri ve C/T'ye bağlı olarak tahmin eden tamamen deneysel sonuçlara dayanan bir korelasyon sunulmuştur.

Anahtar Kelimeler: Katı Süspansiyonları, Bulut Yüksekliği, Yüksek Katı Konsantrasyonu, Uzun Tanklar

Dedicated to my mother, Sevinç Altıntaş, my father, Mehmet Ali Altıntaş,

and my brother, Ege Altıntaş

ACKNOWLEDGMENTS

Foremost, I would like to express my deep and sincere gratitude to my supervisor Assoc. Prof. İnci Ayrancı Tansık for her guidance, patience, motivation, and insight throughout the research.

I would like to thank members of Multi-phase Mixing Research Laboratory, Gökhan Gök, Ahmet Fırat Taşkın, Özge Demirdoğan, Yağmur Özdemir and Usman Kayode Abdulrasaq. They were more than group members for me. I am grateful to them for their friendship and the technical support they supplied whenever I needed it.

I would also like to thank Neslin Güler, Sevil Göktürk, Zeynep Öztan, Salih Ermiş, Ezgi Gözde, Özge Batır, Burak Akdeniz, Elif Kurt, Selin Şengül, Ramazan Umut Dinç, Mehmet Soner Yaşar and Öznur Doğan for their friendship. They have always believed in me and encouraged me throughout the graduate life. I want to express my special thanks to Berkan Atman for his helpful and supportive attitude during the challenging times.

I thank all my dearest friends İdil Dişçi, Zeynep Işılay Başkahya, Hazal Özdemir, Azize Aydın, Gözde Uçak and Beste Şimşek for being there at all toughest and happiest moments of my life.

Finally, I would like to express my deepest love and gratitude to my family Sevinç Altıntaş, Mehmet Ali Altıntaş and Ege Altıntaş. I am grateful for their endless support and love.

This work is financially supported by Scientific and Technological Research Council of Turkey under grant number TUBİTAK 119M684.

TABLE OF CONTENTS

LIST OF TABLES

TABLES

LIST OF FIGURES

FIGURES

LIST OF ABBREVIATIONS

ABBREVATIONS

CH	cloud height (cm)
BG	big glass
MG	medium glass
LG	large glass
PBT	pitched blade turbine
PGM	pressure gage method
SG	small glass

LIST OF SYMBOLS

SYMBOLS

Roman Characters

A'	Ayranci's geometry related constant
C	off-bottom clearance of the impeller (m)
D	diameter of the impeller (m)
d_p	diameter of the particle (μm)
k_E	turbulent energy dissipation rate per unit mass (m^2/s^3)
g	acceleration of gravity (m/s^2)
H	height of the liquid (m)
N	impeller speed (rpm)
N_{js}	just suspended speed (rpm)
N_p	power number
n	exponent on concentration term used in Equation (2)
P	power consumption (W)
S	Zweitering constant
T	diameter of the tank (m)
W	width of the baffles (m)
X	Zweitering's solids concentration (mass of solids/mass of liquid×100)
X_V	solids volume concentration (volume of solids/volume of slurry×100)

Greek Characters

ρ_p	density of the particle (kg/m^3)
ρ_l	density of the liquid (kg/m^3)
$\Delta\rho$	density difference of solid and liquid phases (ρ_p- ρ_l) (kg/m^3)
υ	kinematic viscosity of the fluid (m^2)
τ	torque acting on particle (N.m)

CHAPTER 1

INTRODUCTION

1.1 Definition of Mixing

Mixing is an operation in which two or more components are treated to bring them adjacent to each other as much as possible. In very general terms, objective of mixing may be defined as to reduce the non-uniformity or gradients in terms of concentration, temperature or phases or to initiate a physical or chemical reaction (Atiemo-Obeng et al., 2004).

Multi-phase mixing processes are involved in most industrial applications. Many problems can be encountered in multi-phase mixing due to the complexity of the mixing process in such systems. Improper design of mixing systems or a problem in mixing due to lack of knowledge about the fundamentals of the mixing mechanism may cause great losses in terms of the efficiency of the process. These losses may be quite large considering the large size production vessels. Accurate design of mixing tanks for multi-phase flow applications is critical. The most common types of the multi-phase mixing are explained below.

- Immiscible liquid-liquid mixing is commonly encountered in chemical, petroleum and pharmaceutical industries. These systems comprise of two or more mutually insoluble liquids. These insoluble liquids represent two different phases such as dispersed, or drop, phase and continuous, or matrix, phase. Some examples of these systems are emulsification, nitration, sulfonation and hydrogeneration. The reaction rate in such systems are generally controlled by mass transfer and affected by interfacial area. Therefore, the total surface area of the drop phase affects the mass transfer

and thus the reaction rate. Drop size is an important parameter for such systems. Drop size distribution is affected by impeller type, impeller position, number of impellers and impeller speed.

Industrial process equipment commonly used for liquid-liquid mixing are stirred vessels, rotor-stator mixers, static mixers, decanter, settlers and centrifuges (Leng & Calabrese, 2004).

- Gas-liquid contacting is important for many processes such as chlorination, sulfination, hydrogenation and oxidation. The main objective in gas-liquid contacting is to contact these two phases effectively and efficiently in order to provide mass transfer. Most of the time this becomes challenging due to buoyancy, level rise, bubble coalescence or gas expansion. A good mass transfer may be provided by large interface area between two phases which can be achieved by small bubble size and high gas fraction, and a high mass transfer coefficient. Impeller type, impeller diameter, impeller speed and gas feed rate affect the gas fraction and power consumption in a baffled stirred tank (Middleton & Smith, 2004).
- Solid-liquid mixing operations may be conducted with settling or floating solids. Settling solids have higher density than the liquid whereas floating solids have lower density than the liquid. The main objectives in such operations are to create and maintain a slurry and to enhance the contact between solid and liquid phases. Solid-liquid mixing are known to be carried out in stirred vessels. Axial and mixed flow impellers are suitable for solid-liquid mixing process with settling solids. (Atiemo-Obeng et al., 2004). Solid-liquid mixing that involves settling solids is the focus of this study.

1.2 Solid-Liquid Mixing

Solid-liquid mixing often takes place in the scope of many industrial branches such as polymer processing, biotechnology, pharmaceuticals, automotive, cosmetics and mineral processing. The unit operations in the chemical industry that include solid-liquid mixing are;

- Dispersion of solids
- Dissolution and leaching
- Crystallization and precipitation
- Adsorption, desorption and ion exchange
- Solid-catalyzed reaction
- Suspension polymerization

All these unit operations except dispersion of solids involves mass transfer between solid and liquid phases. This emphasizes the importance of the contact between two phases in a solid-liquid mixing process.

In solid-liquid mixing there are two main focuses: solids suspension and solids distribution.

1.2.1 Solids Suspension

Solids suspensions are mainly focused on the motion of the solid particles on the bottom of the tank. In most solids suspension applications, the main objective is to provide maximum contact area between solid and liquid phases with minimum power consumption. This objective is satisfied as the operation is carried out at the impeller speed that is equal to just-suspended speed (N_{js}). Thus, one of the key parameters in solids suspension is N_{js}, at which no particle remains stationary on the bottom of the tank for more than 1 or 2 seconds (Zwietering, 1958).

There are several methods to determine N_{js}. The most common method is *observing the motion of the solids from the tank bottom.* This method requires a tank with a

transparent bottom. The solids are observed as impeller speed is increased gradually until no solids remain stationary more than 1 or 2 seconds.

Another way to determine N_{js} is *pressure gage method (PGM)*. In this method, a pressure transducer is attached to the bottom of the tank. The impeller speed is increased gradually during the process. Pressure transducer measured the pressure at the bottom of the tank at each impeller speed, and total pressure data obtained. The pressure change at the complete off-bottom suspension condition is determined. The difference between this value and total pressure data equals to dynamic head effects. The change in pressure data only with increasing number of suspended solids is obtained by subtracting the dynamic head effects from the total pressure data. Intersection of this curve and the pressure change at the complete off-bottom suspension condition equals to just-suspended point. The impeller speed at this point is N_{js} (Kutukcu & Ayranci, 2019).

For cases in which running experiments is not possible, there exist *models that predict N_{js}* in literature. Zwietering (1958) was the first to propose a model that predict N_{js}.

$$N_{js} = S\left[\frac{g(\rho_s - \rho_l}{\rho_l}\right]^{0.45} \frac{\upsilon^{0.1} X^{0.13} {d_p}^{0.2}}{D^{0.85}} \qquad (1)$$

Zweitering's model has been used as a design equation for solids suspension operations in industrial applications. Besides this pioneering work, there are some other studies in literature that proposed a model that predicts N_{js}. Baldi et al. (1978) proposed a model based on a theory that the potential energy which is required to lift a particle equals to the turbulent kinetic energy transferred to the particle. They also stated that the turbulent kinetic energy should be the energy of the turbulent eddies which have similar sizes as the particle. Davies (1986) also proposed a model using this energy balance theory. In Davies' model the solids concentration term is slightly more pronounced then Baldi's model. The concentration term in Davies' model

represents the assumption that particles that are suspended distribute energy, and this energy causes the turbulence to decrease.

Recently Ayranci & Kresta (2014) examined the model that was proposed by Zwietering (1958), and showed that this model is only applicable up to solids concentration of 2 wt%. They proposed a new model by considering Baldi's hypothesis. The model is applicable for a wide range of solids concentrations and successful in scale-up:

$$N_{js} = A'\left[\frac{g(\rho_s - \rho_l}{\rho_l}\right]^{0.5} \frac{d_p^{\frac{1}{6}} X^n}{N_p^{\frac{1}{3}} D^{\frac{2}{3}}} \frac{T}{D} \qquad A' = S \frac{d_p^{\frac{1}{30}} N_p^{\frac{1}{3}} \upsilon^{0.1}}{D^{\frac{11}{60}}} \frac{D}{T}\left[\frac{g\Delta\rho}{\rho_l}\right]^{-0.05} \qquad (2)$$

The exponent on the solids concentration in this model, which appears as n, has three possible values based on the particle groups that were tested: 0.17, 0.23 and 0.32. An exponent of 0.23 can be used as an average exponent that represents the entire data set.

Based on the motion of the solids at the bottom of the tank, there are three degrees of solid suspension. A schematic representation of the three degrees of a solid suspension is given in Figure 1.1**.**

- Partial suspension enables solids to move but not all parts of the solids contact with liquid phase since some portion of the solids remains stationary on the bottom. The partial suspension is also known as on-bottom motion. Impeller speed at this condition is lower than N_{js}. This condition is not compatible for most chemical processes due to limited contact of solid and liquid phases.
- Complete suspension, also known as off-bottom suspension, is the most commonly used suspension degree for solid-liquid mixing operations in industrial applications. It allows entire surface area of the solids to contact

with the liquid at the minimum power consumption. This degree of suspension is based on the Zwietering criterion (Zwietering, 1958). Hence, impeller speed at this condition is N_{js}.

- Uniform suspension enables all solids to be distributed uniformly throughout the tank. While this suspension condition may be necessary for some applications, for example crystallization and precipitation, it is not widely applied due to speed and power limitations.

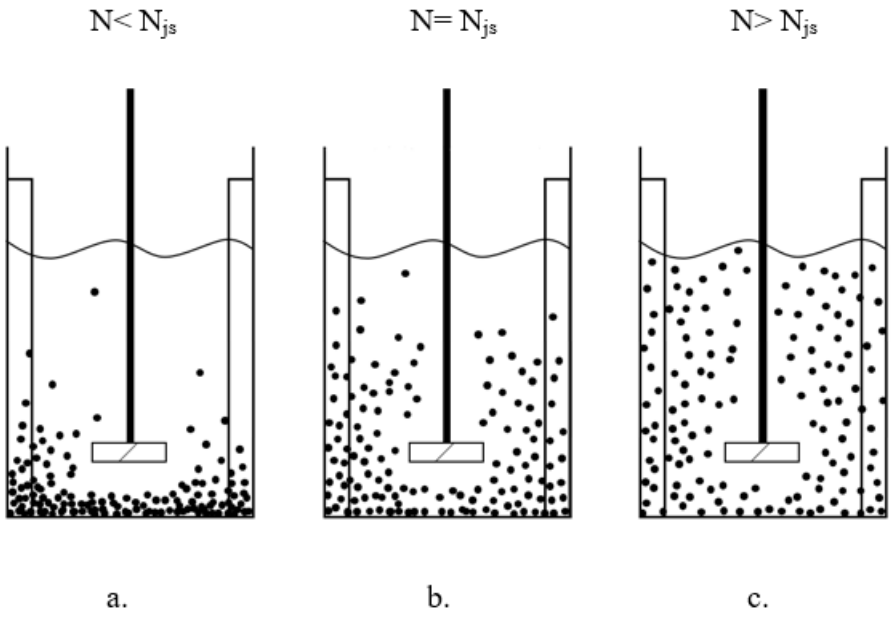

Figure 1.1. (a) Partial suspension, (b) Complete suspension, (c) Uniform suspension

The degree of suspension is selected based on the requirements of each process under consideration. For example, partial suspension is sufficient for dissolution of highly soluble solids yet they are generally not suitable to achieve an efficient chemical reaction or heat and mass transfer process.

1.2.2 Solids Distribution

The second main focus in solid-liquid mixing operations is *solids distribution*. The distribution of the solids in stirred vessels is analyzed in two dimensions: radial and axial. Analysis of the radial distribution of the solids focuses on the investigation of the change in the concentration of the solids along the distance from the center towards the wall of the tank. Similarly, analysis of the axial distribution of the solids focuses on the investigation of the change in the concentration of the solids along the liquid height. In this study, the axial distribution of the solids in a stirred tank is investigated. One of the key parameters in identifying the axial solids distribution is cloud height.

At high solids concentrations a distinct level to which most of the solids are suspended appears. Two parts can be identified by this level. Figure 1.2 shows the schematic representation of these two parts. The part that is below this level is solid-rich while the part above this level is liquid-rich. The height of the interface that appears between these two parts is called the *cloud height*.

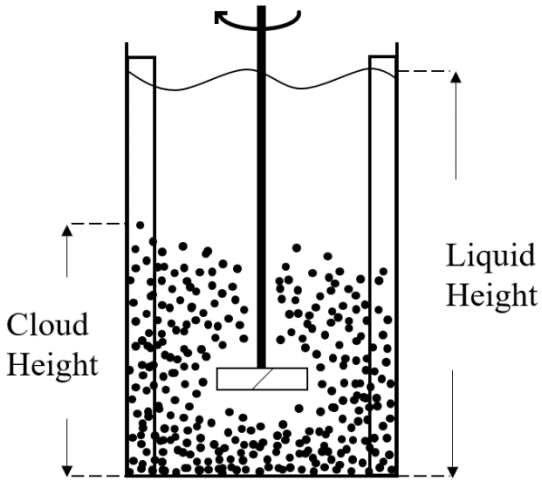

Figure 1.2. Schematic representation of cloud height

Beyond the solid-rich part, only occasional visits of a small portion of solids occur. The most efficient solid-liquid mixing takes place in the solid-rich part. It is; therefore, desired to keep the solids rich part as large as possible. If there is any fluid that is not in contact with the solids rich part this causes large production losses. Accurate measurement and prediction of cloud height can prevent such losses.

1.2.2.1 Determination of Cloud Height

Cloud height can be determined by several methods. The most common measurement method is visual *observation*. In order to measure cloud height visually a tank with transparent walls is required. Due to fluctuating nature of the interface, the visual measurement of cloud height is not straightforward. Cloud height is measured when the observer makes sure the level of the cloud height is at the eye level. Nevertheless, there is no defined certain measurement point for cloud height. This causes large discrepancies in measurements obtained by different observers. Identification of a universally accepted measurement point for cloud height can eliminate this problem.

Cloud height can also be measured using *optical methods*, e.g. optical attenuation technique, ultrasound velocity profiler technique. Installing a probe aligned vertically on the top of the stirred tank, a concentration or a velocity distribution along the axial plane is obtained depending on the selected technique. The level above which solids concentration drops dramatically is determined from the concentration profile obtained using an optical method (Ochieng & Lewis, 2006). The height of this level corresponds to cloud height. Similarly, the level above which the axial velocity profile direction distinguishes is determined from the obtained axial velocity profile. The direction of the axial velocity profile changes due to a weak circulation loop in the liquid-rich region (Sardeshpande et al., 2010). The height of the level above which the direction of the velocity changes corresponds to cloud height.

Image analysis is another method used for measurement of cloud height. In this method, experiments are recorded. The recorded video is then processed to bring the brightness and the contrast to a desired level. If sufficient light is provided above the stirred tank, the light intensity is observed at its maximum level on the interface between solid-rich and liquid-rich parts. After selecting a suitable software, cloud height is measured by determination of the height of the level at which light intensity reaches its maximum value (Sardeshpande et al., 2010).

For cases in which running experiments is not possible, such as the design step, a model that predicts cloud height may be preferred to determine cloud height. There is only one study that propose a model that predict cloud height in literature (Bittorf & Kresta, 2003). This model predicts cloud height as a function of impeller speed and tank geometry. Recently, in a conference presentation Brown (2018) proposed a model for cloud height prediction which is a function of solids concentration, particle properties, tank geometry and impeller speed; however, the exponents on the parameters related to the particle properties were not revealed explicitly.

1.3 Determination of Power Consumption

There are two methods for calculation of power consumption: the torque method and the turbulent dissipation method. In the torque method, the power consumption by the impeller can be calculated from

$$P = 2\pi N\tau \tag{3}$$

In the turbulent dissipation method, dissipation rate of the turbulent kinetic energy in a stirred tank is integrated. Total amount of the energy dissipation in the tank should be equal to energy input to flow. Thus, power consumption can be calculated from

$$P = \rho \int k_E \, dV \tag{4}$$

The torque method is more accurate that the turbulent dissipation method. Thus, the torque method is recommended (Kresta et al., 2016). In this study, the torque method was used for power consumption calculations.

1.4 Motivation of Thesis

In literature, the current definition of cloud height has unclear points that may cause remarkable inconsistencies between different studies. One of these unclear points is the non-existence of a certain measurement point of cloud height. Besides, the current definition of cloud height does not involve limitations on the parameters such as solids concentration and impeller speed although it has been several times proven that no interface forms at low solids concentrations and impeller speeds.

Similar to solids concentration and impeller speed, there is another factor that influence cloud height: particle properties. In literature there is no model that predicts cloud height as a function of solids concentration or particle properties.

The aims of this study are to enhance the current definition of cloud height by determination of a certain measurement point of cloud height and determination of limitations on solids concentration and impeller speed, to investigate the effects of solids concentration and particle properties on cloud height and to propose a model that predicts cloud height as a function of these parameters.

CHAPTER 2

LITERATURE SURVEY

Musil (1984) was the first to recognize the formation of two distinct parts appeared as solid-rich and liquid-rich in a non-homogeneous solid-liquid mixing tank. This study was carried out at high solids concentrations, between 4-14 vol%, at just suspended condition. It was observed that the liquid-rich part stayed almost unmixed relative to the solid-rich part, and deprived of particles. Similarly, Kraume (1992) and Bujalski et al. (1999) stated very poor mixing beyond the interface that was observed at high solids concentrations. Bittorf & Kresta (2003) measured the velocity using Laser-Doppler Velocimetry in only liquid phase and they combined the findings with cloud height data found in literature. They also measured the velocity in liquid-rich part above the solids cloud in order to investigate the turbulence dampening due to existence of solid particles, and stated that the liquid-rich part was only occasionally visited by a small portion of solids. Recently, Ayranci & Kresta (2021) investigated the turbulence decay in the upper part of the tank at high solids concentrations, and they found the turbulence decay beyond the maximum level that solids reach was constant and nearly zero. These emphasize that the mixing essentially occurs in the solid-rich part of the stirred tank. An interface forms between the solid-rich and the liquid-rich parts. The height of the solid-rich part provides information about the region in which the mixing mainly occurs. The height of the interface that forms between the solid-rich and the liquid-rich parts at high solids concentrations is defined as cloud height (Bujalski et al., 1999; Bittorf & Kresta, 2003; Kasat et al., 2008; Sardeshpande et al., 2009). However, some studies recognized cloud height as the height to which solids are suspended (Hicks et al., 1997; Lassaigne et al., 2016). This might be due to the fact that the definition of

cloud height is ambiguous in terms of measurement point, and is lack of limitations on parameters that affect cloud height, such as solids concentration and impeller speed. The studies that investigated cloud height were reviewed in terms of the parameters that affect the definition of cloud height., and they are presented in the following subsections.

2.1 Measurement Point of Cloud Height

Only a limited number of studies in the literature reports the measurement point of cloud height determined by visual observations. Sardeshpande et al. (2009) reported the arithmetic mean of the lower and upper limits of cloud height across the diameter of the tank due to variations. Bujalski et al. (1999) recorded cloud height data at the minimum height of the interface. Eng et al. (2015) stated that the data has been taken at the location closest to the windward side of the baffle when the impeller rotated in clockwise direction. Similarly, the information about the measurement point of cloud height determined by other methods was also presented by a limited number of studies. Ochieng & Lewis (2006) determined the cloud height using optical attenuation technique. They reported the data at the inflection point on the curve representing the variation of volume fraction with axial distance as cloud height data. Kasat et al. (2008) stated that the cloud height they measured was the distance of the highest point of the iso-surface of the average solids concentration. A recent study proposed a new method of cloud height measurement that was based on the image analysis (Xu et al., 2019). In this method, the boundary of the liquid-rich and solid-rich zones were determined getting the matrix of pixels and extracting the colors of red, green and blue. Then, for one selected column of the pixel matrix along the height of the tank, the point at which the color components stopped varying was detected to be identified as cloud height. In this method, a working zone was selected on the images of the mixing process. The authors selected a region near to the central axis of the tank as the working zone. These are not sufficiently clear statements of measurement points, and they are not easy to visualize and reproduce.

One may assume the particle cloud in a mixing operation is a solid bulk with a flat interface and easy to measure visually; however, the reality is different. Sardeshpande et al. (2009) and Eng et al. (2015) observed that cloud height is not a flat interface across the tank diameter and it also varies with time. A recent study by Ayranci & Kresta (2021) stated that an inclined shape of cloud height was observed as a 45º PBT was rotating, and this created variations between cloud height data across the tank. They showed that cloud height measured at different locations, such as in front of the baffle, back of the baffle, or mid-plane, significantly differed. Thus, the non-existence of a clearly defined measurement point for the cloud height in literature is an important issue considering the fact that the cloud height measurements depend on the observer. Observer dependent errors are always present among data reported by different observers, and these errors are even larger when the measurement point is not a universally accepted point.

2.2 The Limitations and Effects of Solids Concentration and Impeller Speed on Cloud Height

Several studies proved that solids concentration and impeller speed affect cloud height. The research on these two parameters is reviewed separately below.

2.2.1 The Limitations and Effects of Solids Concentration on Cloud Height

In the studies investigated the effect of solids concentration on cloud height, both weight and volume percent were used to express the solids concentration. Some of the studies comprise of a wide range of solids concentration starting from very low values, even though cloud height is expected to occur at high solids concentrations. Hicks et al. (1997) reported the change in cloud height with solids concentration between 0.5-50 wt%. This data begins from a very low solids concentration value. Similarly, Sardeshpande et al. (2009) reported cloud height data at 1 vol% although

they stated that particles were observed to be distributed throughout the tank at this concentration, which means no interface was observed. This shows that some of the studies in literature considered the cloud height as the height to which solids could reach regardless of the formation of an interface. These are not in line with the rest of the literature since cloud height was described as the height of the interface formed between solid-rich and liquid-rich parts at high solids concentrations. According to this, an interface between solid-rich and liquid-rich parts of the vessel should form in order to record cloud height data. This interface forms at high solids concentrations. In the study of Bujalski et al. (1999) cloud height was also expressed as 'interface height' and cloud height data were recorded at solids concentrations varying between 20-40 wt%. In the study of Micale et al. (2004) at a low solids concentration of 1.4 vol% an interface did not form and all particles were reported to be distributed throughout the tank. Thus, they reported cloud height data at higher solids concentrations. There are deficiencies in cloud height definition in terms of solids concentration as such there is no established lower limit of solids concentration. Consequently, the definition of cloud height might be interpreted differently by different researchers. This may be the reason that some of the studies in literature reported cloud height data at low solids concentration in which no interface forms. There is a need for clarification of the definition of cloud height in terms of solids concentration. An identification of the lower limit of solids concentration and a threshold limit which indicates a persistent, universally acceptable cloud height occurrence is required.

Some studies in literature investigated the effect of solids concentration on cloud height at high solids concentrations at which an interface could be formed. According to images presented by Micale et al. (2004), cloud height first decreased and then stayed almost constant with increasing solids concentrations between 0.48-14.48 vol % at a fixed impeller speed. Hicks et al. (1997) also found that at higher solids concentrations, cloud height did not significantly change with an increase in solids concentration, at an impeller speed of N_{js} for each concentration. Bujalski et al. (1999) concluded that cloud height was almost the same for each concentration

between 20-40 wt%. However, Ochieng & Lewis (2006) reported a linearly decreasing cloud height profile with increasing solids concentration within the range of 3-20 wt%. Similarly, Eng et al. (2015) observed a linear decrease in cloud height as solids concentration was increased within the concentration range of 2.5-15 vol%.

The inconsistencies between different studies that investigated the effect of solids concentration on cloud height may be originated from the fact that these studies measured cloud height at different degrees of solids suspension. In some of the studies reviewed above, the cloud height data for different solids concentrations were recorded at a fixed impeller speed that was chosen for the slurry under investigation (Bujalski et al., 1999; Micale et al., 2004; Matthias Eng, Rasmus Jonsson, 2015). The impeller speed is an important parameter that determines the degree of suspension. At an impeller speed that was not selected based on a criterion, the slurries that have different solids concentrations may be at different degrees of suspension. Thus, the results of the cloud height investigation of slurries at different conditions are expected to differ significantly.

2.2.2 The Limitations and Effects of Impeller Speed on Cloud Height

The effect of impeller speed on cloud height was proven to be significant by many studies in literature. Bujalski et al. (1999) identified five suspension stages depending on the impeller speed. The observations began at low impeller speeds. The impeller speed was increased as stages proceeded. At the first stage, which was at very low impeller speeds, a small portion of solids was seen to be lifted up and reached the liquid surface. The second stage was designated as the stage in which an interface between solid-rich and liquid-rich parts of the tank was observed. At the third stage, the height of the interface was seen to decrease. The fourth stage was the observation of an increase in cloud height with a further increase in impeller speed. At the last stage, no interface was observed. According to this study, at low impeller speeds an interface between solid-rich and liquid-rich parts of the tank does not form; therefore, it is not possible to record a meaningful cloud height data at low impeller

speeds. Similarly, Hicks et al. (1997) did not include any data below approximately 0.3 N/N_{js}. On the other hand, Lassaigne et al. (2016) reported cloud height data at very low speeds, even at 0 rpm, although it was shown as an image that no particles were suspended. The reason behind the inconsistencies between different studies in literature is the absence of the lower limit of solids concentration in the current definitions of cloud height.

The studies investigating the effect of impeller speed on cloud height can be divided into two groups as observing monotonic and non-monotonic behavior of cloud height. Sardeshpande et al. (2009) observed non-monotonic behavior of cloud height when impeller speed increased, similar to the above-mentioned Bujalski et al. (1999). However, Hicks et al. (1997), Ochieng & Lewis (2006), Hosseini et al. (2010) and Eng et al. (2015) reported a monotonic behavior - the cloud height increased linearly with increasing impeller speed. The correlation proposed Bittorf & Kresta (2003) also gives a monotonic relation between the cloud height and the impeller speed.

2.3 The Effect of Particle Properties on Cloud Height

In a number of investigations, the effect of particle properties on the solids distribution in stirred tanks was observed. Hosseini et al. (2010) studied the homogeneity of solid-liquid systems in which solids could not be distributed throughout the vessel, and interpreted cloud height as a concept that represented homogeneity. Cloud height was only investigated at increasing impeller speeds; it was not investigated in terms of particle properties. However, the effect of particle properties on the homogeneity was investigated (for particle size between 100-900 μm and specific gravity of the particle between 1.4 and 6). It was found that the homogeneity decreased due to increasing particle size and density. Although cloud height is not the homogeneity, this might indicate that particle properties might influence cloud height as well as influence the homogeneity. A recent study of Ayranci & Kresta (2021) investigated the turbulence decay in the upper part of the

tank at high solids concentrations, and found that particle properties is an important parameter for solids cloud height. The analysis was performed using glass beads with the sizes of 140 and 521 μm.

A limited number of studies in literature investigated the effect of particle properties on cloud height. Sardeshpande et al. (2010) aimed to investigate the variations of cloud height with impeller speed and particle properties. Glass beads of 50 μm and 250 μm were used as particles. During experiments, they realized that the slurries of 50 μm particle form a 'milky' appearance throughout the tank. This made the observations challenging due to not being able to track the interface. Thus, the study was conducted using only 250 μm particle. In this study, the effect of particle size on cloud height was not reported quantitatively, yet it was pointed that the particle size affected the dynamics within the cloud, as such the form of the solid cloud varied. Bujalski et al. (1999) investigated the effect of particle size on cloud height at increasing impeller speeds. The particle size was varied between 115 and 678 μm. Expectation of the authors from this investigation was to observe a decreasing cloud height profile due to increasing particle size. The results met the expectation only at high impeller speeds. Similarly, Eng et al. (2015) studied the effects of particle size on cloud height at changing impeller speed and solids concentration. For this analysis, particles with sizes of 0.5, 1 and 2 mm were used. The authors reported that cloud height increased with decreasing particle size. Hicks et al. (1997) investigated the effect of particle properties on cloud height for a wider range of particle size and density compared to the rest of the literature. Cloud height data of various particles (particle size between 600-2950 μm and particle density between 1053-2590 kg/m^3) were investigated at increasing impeller speeds. The authors stated that particle properties did not affect cloud height significantly. Cloud height data of all particles except an extremely rapidly-settling particle was observed to be almost the same. In this study, the effect of the density of particle was not investigated using particles that had similar sizes but different densities. That is, the variations of cloud height merely with particle density was not presented.

These studies investigated the effect of particle properties on cloud height at increasing impeller speed or solids concentration, yet the relation between the particle properties and cloud height was not analyzed thoroughly.

2.4 The Effect of Off-bottom Clearance on Cloud Height

Several studies in literature investigated the effect of off-bottom clearance on cloud height. These studies performed this analysis at increasing impeller speeds or at a fixed impeller speed or at N_{js}. Musil (1984) investigated the change of cloud height due to increasing off-bottom clearance at increasing impeller speed. The author stated that cloud height almost did not change with off-bottom clearance low impeller speeds. After a minimum value of impeller speed was exceeded, cloud height increased as off-bottom clearance was increased. This was observed for five different off-bottom clearance values. This minimum speed was found to be very close to N_{js} values determined experimentally. This analysis led to the investigation of the effect of off-bottom clearance on cloud height at N_{js}, and cloud height was observed to increase with increasing off-bottom clearance. Similarly, Hicks et al. (1997) and Špidla et al. (2005) found that cloud height decreased with decreasing off-bottom clearance at N_{js}. On the contrary to the findings of these studies, the model that was proposed by Bittorf & Kresta (2003) propounded that cloud height is inversely proportional to off-bottom clearance.

Hosseini et al. (2010) investigated the effect of off-bottom clearance on homogeneity with three different off-bottom clearance values at a fixed impeller speed. A non-monotonic variation of cloud height with increasing off-bottom clearance was observed. Homogeneity first increased and then decreased with increasing off-bottom clearance. It should; however, be noted that the homogeneity is not equivalent to the cloud height.

Jafari et al. (2012) studied the effect of off-bottom clearance on axial solids concentration at a fixed impeller speed. The authors stated that suspension of solids

could be achieved at lower impeller speeds when off-bottom clearance was set at a lower value, but solids could not be distributed to higher levels. A non-monotonic variation of cloud height with increasing off-bottom clearance was observed. Cloud height was found to increase with increasing off-bottom clearance at low impeller speeds. However, cloud height was observed to almost stay constant as off-bottom clearance was increased at high impeller speeds. Zhao et al. (2014) also studied the effect of off-bottom clearance on cloud height at a constant impeller speed. Different from the studies mentioned above, in this study, an improved Intermig impeller was used. They reported that cloud height decreased as the off-bottom clearance was increased similar to the model that was proposed by Bittorf & Kresta (2003) propounded.

Inconsistencies are observed between the results of the studies in the literature. This may originate from the fact that off-bottom clearance affects cloud height disparately at different degrees of suspension or at different ranges of impeller speed.

2.5 Models that Predict Cloud Height

Bittorf & Kresta (2003) proposed a model that predicted cloud height as a function of impeller speed and tank geometry. This model was formed based on the velocity decay in three-dimensional wall-jets. They combined their measurements of core velocity of the wall jet and existing cloud height data in literature at that time in order to create the model. They stated that the model was not in a good agreement with the fast settling particles, which had terminal velocity higher than 0.173 m/s, and the model was applicable for predicting cloud height between 0.6 and 0.8 CH/H. The model proposed by Bittorf & Kresta (2003) is given below.

$$\frac{CH}{T} = \frac{N}{N_{js}}\left[0.84 - 1.05\frac{C}{T} + 0.7\frac{(D/T)^2}{1-(D/T)^2}\right] \quad (5)$$

Ochieng & Lewis (2006) performed similar analysis with Bittorf & Kresta (2003) using a particle that had larger density, although they did not propose a model that predicts cloud height. They found a similar relation between cloud height and the velocity measurements; however, the constants were found lower than the constants in the analysis performed by Bittorf & Kresta (2003). This shows that particle properties affect cloud height, and thus, a model that predicts cloud height should involve a parameter that represents particle properties.

Recently in a conference Brown (2018) presented a model that predicted cloud height as a function of solids concentration, particle properties, tank geometry and power consumption. However, the exponents on the parameters related to the solids concentration, particle properties and off-bottom clearance were not revealed. Therefore, there is still no available model that predicts cloud height as a function of solids concentration, particle properties and off-bottom clearance.

CHAPTER 3

EXPERIMENTAL PROCEDURE

3.1 Experimental Setup

The experiments were conducted in two setups: Setup 1 and Setup 2. These two setups consisted of cylindrical flat-bottom tanks with a diameter (T) of 0.24 m. In both tanks, four equally spaced baffles with width (W) of T/10 were used. A 45° down-pumping pitched blade turbine (PBT) with a diameter (D) of T/3 was used. Geometrical features of the setups are given in Figure 3.1.

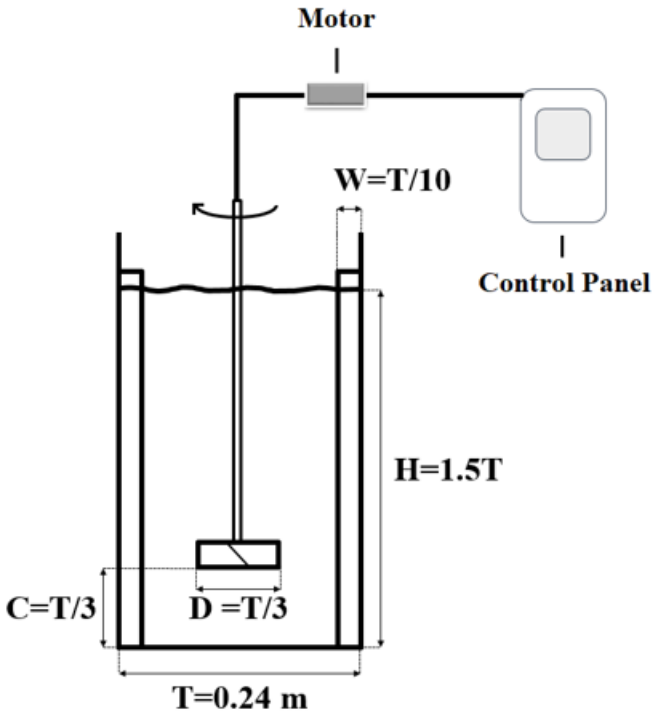

a.

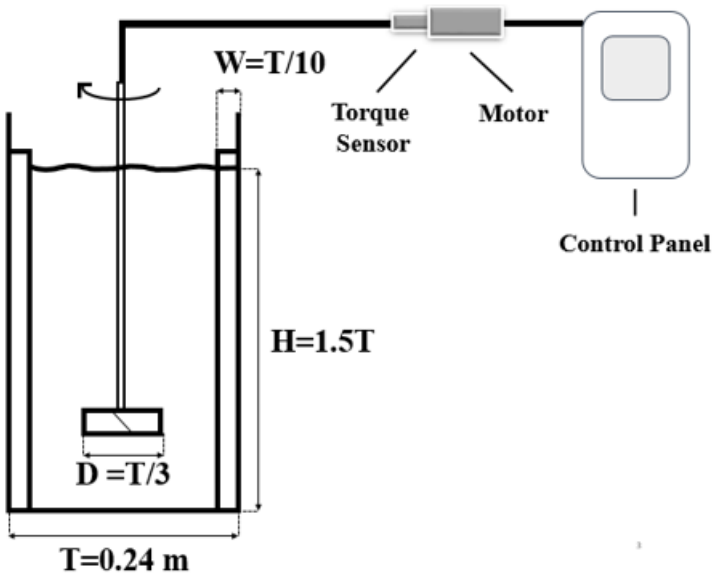

b.

Figure 3.1. Geometrical configuration of (a) Setup 1 (b) Setup 2

Off-bottom clearance, C/T, could be adjusted in Setup 2, but not in Setup 1. In Setup 1, off-bottom clearance was set as T/3 as seen in Figure 3.1a. Setup 1 consisted of a tank that had a transparent bottom. N_{js} values of the corresponding cases were determined by visual observations of the bottom of the tank. The liquid height (H) was equal to 1.5T in the majority of the experiments performed in this study. Besides those experiments, several experiments with H=T were also performed in Setup 1.

A Servo motor was placed above the tank. A control panel were located at one side of Setup 1. This panel enabled to adjust impeller speed and rotation direction, and to stop the system immediately for any possible emergency.

In Setup 2, the tank had an opaque bottom; therefore, N_{js} could not be observed visually. N_{js} was predicted using a model that predicts cloud height accurately up to solids concentration of 35 wt% (Ayranci & Kresta, 2014). The liquid height (H) was equal to 1.5T in the majority of the experiments. Several experiments with H=T were also performed in Setup 2.

A Servo motor which was connected to a torque sensor was placed above the tank. Sensor and the motor were connected to a control panel as seen in Figure 3.1b. Control panel enabled adjusting impeller speed and the direction of the rotation, and recording torque data. This panel had also an emergency button for any possible danger.

3.2 Materials

Solid particles used in experiments were glass beads in four different sizes, Al_2O_3, Garnet, and Steel. Physical properties of all particles are given in Table 3.1. Glass beads were named based on their sizes. Abbreviations of their names can be seen in Table 3.1. Names of the rest of the particles were not abbreviated.

Table 3.1 Physical properties of particles used in this study

	ρ_p (kg/m^3)	d_p (μm)
Small Glass (SG)	2500	123.6
Medium Glass (MG)	2500	200.4
Large Glass (LG)	2500	573.9
Big Glass (BG)	2500	711.7
Al_2O_3	3700	217.1
Garnet	4000	221.7
Steel	7600	177.0

Densities of the particles were determined using a pycnometer. Given values were calculated by dividing the mass of the solids by the volume of the solids. The volume of the void between particles was not included; therefore, the given density is particle density, not the bulk density. Density measurements were performed twice. Arithmetic mean of two measurements was reported. The sizes of the particles were determined using a Malvern Mastersizer 3000 instrument. For each analysis, the instrument was adjusted to perform five times. Arithmetic mean of number mean

diameter (d_{50}) was recorded as the size of corresponding particle. Each measurement was repeated twice. Arithmetic mean of two measurements were reported.

Densities of SG, MG, LG and BG were the same, yet the sizes were different. Al_2O_3, Garnet, Steel and MG had similar sizes, yet the densities were different as seen in Table 3.1.

The liquid used in all experiments was tap water.

3.3 Experimental Procedure

Cloud height was measured visually in all the experiments. Cloud height is a fluctuating interface. In all of the measurements it was ensured that the fluctuating interface was at the eye level of the observer. A cloud height measurement required an observation lasted 1 to 3 minutes. Every cloud height measurement was repeated three times. The reported cloud height data is the arithmetic mean of the three measurements. Necessary lighting was provided from the top of the tank.

In this study, N_{js} values were obtained by visual observation of the tank bottom for each type of particle at each solids concentration for the experiments in Setup 1. Measurements were started from a low impeller speed. The impeller speed was increased gradually until no particle was observed to remain stationary more than 1-2 seconds. After each impeller speed was set, the system was left for 2-3 minutes to reach steady state, then N_{js} observation was conducted. Measurement of N_{js} was also repeated 3 times. Arithmetic mean of three measurements was reported as N_{js} data.

3.3.1 Experiments on Cloud Height Definition

Different experiments were performed in order to develop the necessary criteria for a clear definition of the cloud height. In this sub-section the procedures of these experiments are detailed.

3.3.1.1 Identification of Measurement point of Cloud Height

In identifying the most meaningful measurement point for cloud height dye experiments were used. Red food dye was injected by a peristaltic pump into the tall tank which contained either single-phase (water) or slurry. Density and viscosity of the liquid phase were assumed not to change during the process since the food dye was diluted with water before injection. Single-phase system consisted of only water, slurry system consisted of 6.06 vol% (~6 vol%) MG slurry. The dye injection point was the same for both single-phase and slurry system, as shown in Figure 3.2. This point corresponded to the solid-rich volume for the slurry system. For both systems impeller speed was set at the same value, which was the N_{js} of 6 vol% MG slurry. The dye injection process was recorded using OSMO Action camera. Comparison of the snapshots obtained from the two systems were used to identify the most meaningful cloud height measurement point.

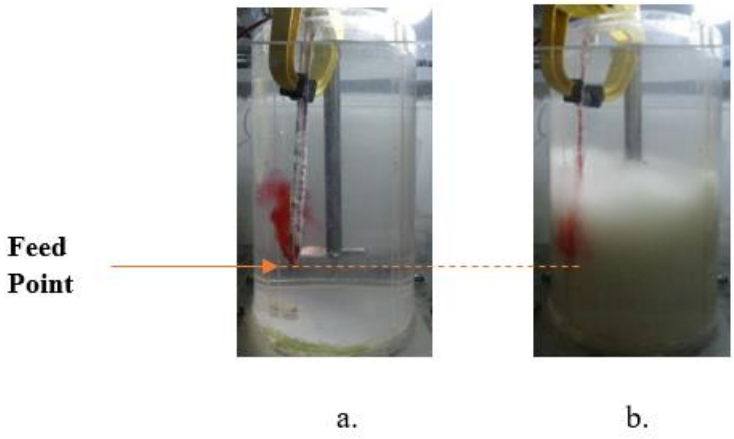

Figure 3.2. Food dye injection into (a) single-phase and (b) slurry

Once the measurement point was determined, cloud height was measured using MG slurries for H=T and H=1.5T. Limited number of experiments was performed in tanks with H=T. The tests at H=T were performed at solids concentrations varying

between 5–25 vol% at N_{js}. The majority of experiments was performed in tanks with H=1.5T. These tests covered a range of solids concentrations varying between 0.5-25 vol% and a range of impeller speeds varying between 0.8-1.5 N_{js}.

3.3.1.2 Investigation on Limitations and Effects of Solids Concentration and Impeller Speed

The limits of solids concentration and impeller speed on the measurement of cloud height was investigated using MG slurries. Once the limits were identified using MG slurries, a particle with different size, but the same density (LG) and a particle with different density, but the similar size (Garnet) were tested. These tests were performed at the same solids concentration range or at the same N/N_{js} range, in which MG experiments were tested. All the measurements for these tests were done at the fixed measurement point identified using the dye tests.

The solids concentration limit to observe a clear interface was investigated at N_{js} for fifteen different solids concentrations ranging between 0.5–25 vol% MG slurry. After each solids loading, the system was left for 2-3 minutes to reach steady state, then the cloud height was measured. Impeller speed limits to observe a clear interface between solid-rich and liquid-rich volumes was determined with 5 vol% MG slurry. The tests started from $N=0.06N_{js}$ and gradually increased up to $N=1.5N_{js}$ with approximately 25 rpm increments. After each increment the system was left for 2-3 minutes to reach steady state, then the cloud height was measured. Videos were recorded, and snapshots were taken by OSMO Action camera.

3.3.2 Experiments on Effects of Solids Concentration on Cloud Height

Analysis of the effects of solids concentration on cloud height was performed using slurries of SG, MG, LG, BG, Al_2O_3 and Garnet at N_{js}. In the experiments with glass beads, solids concentration was varied between 2 and 25 vol%. In the experiments

with Al_2O_3 and Garnet, solids concentration was varied between 2 and 20 vol%. For this analysis, liquid height was fixed at 1.5 times of tank diameter.

3.3.3 Experiments on Effects of Impeller Speed on Cloud Height

Analysis of the effects of impeller speed on cloud height was performed using slurries of SG, MG, LG, BG, Al_2O_3 and Garnet at 0.8, 1, 1.2, 1.3 and 1.45 N/N_{js}. All experiments in this analysis were conducted with 5 vol% slurries. Steel could not be involved in this analysis since very high impeller speeds were required due to its high density. For this analysis, liquid height was fixed at 1.5 times of tank diameter.

3.3.4 Experiments on Effects of Particle Properties on Cloud Height

To investigate the effect of particle diameter, glass beads in four different sizes (SG, MG, LG and BG) were used. The sizes of the particles were given in Table 3.1. The experiments were performed at varying solids concentration between 2-25 vol%. The measurements were obtained at N_{js} of corresponding particle at corresponding solids concentration.

The effect of density of the particle on cloud height was investigated using slurries of MG, Al_2O_3, Garnet and Steel. The experiments were performed at 2 and 5 vol % and at N_{js}. This analysis was also performed at varying solids concentration between 2-25 vol% for slurries of MG, Al_2O_3 and Garnet. Experiments were performed at N_{js} of corresponding particle at corresponding solids concentration.

In the experiments on the analysis of the effects of particle properties on cloud height, liquid height was fixed at 1.5 times of tank diameter.

3.3.5 Experiments on The Analysis of Effects of Off-Bottom Clearance on Cloud Height

Effects of off-bottom clearance on cloud height was examined by using slurries of SG, MG, LG, BG, Al_2O_3 and Garnet. All experiments in this analysis were conducted with 5 vol% slurries. For this analysis, C/T values were set at 0.167, 0.25 and 0.33. The majority of experiments were conducted at N_{js} in a system in which liquid height was equal to 1.5 times of tank diameter. Limited number of experiments were performed at $N< N_{js}$ and $N> N_{js}$ using 5 vol% slurries of LG, BG and Garnet. Besides, limited number of experiments in a system in which liquid height was equal to tank diameter was also performed.

Until this part of the study, all N_{js} values were determined using the transparent bottom of tank in Setup 1. In this setup, C/T was fixed at 0.33. Thus, all N_{js} values determined by visual observation was for C/T=0.33. For the analysis of the effects of off-bottom clearance on cloud height, Setup 2 was used. In this setup, N_{js} values could not be determined by visual observations due to non-transparent bottom of the tank. N_{js} for different C/T values were determined using one of the models that predict N_{js}. The model that was proposed by Ayranci & Kresta (2014) was used. This model is given in Equation ((2). Ayranci & Kresta (2014) proposed three different exponents for solids concentration parameter in the model for different particle groups. These exponents are 0.17, 0.32 and the arithmetic mean of these two exponents, 0.23. To find the most suitable exponent for each particle, N_{js} values that were obtained from the experiments in Setup 1 were compared with N_{js} values predicted by this model. For each particle, the exponent that fitted the best was selected to be used for the experiments in Setup 2. N_{js} values of all particles except SG was fitted very well to the model with the exponent of 0.17. N_{js} values of SG was found to be fitted very well to the same model but with an exponent of 0.13. This exponent was similar to the exponent of solids concentration of the model proposed by Zwietering (1958), but the model that was used belonged to Ayranci & Kresta (2014).

3.3.6 Experiments on The Analysis of Power Consumption

Analysis of power consumption was performed at 0.8, 1, 1.2, 1.3, and 1.45N/N_{js}. This analysis was done by recording torque in Setup 2. The experiments were performed using 5 vol % slurries of SG, MG, LG, BG, Al_2O_3 and Garnet at a fixed off-bottom clearance of T/3.

At each impeller speed, torque was recorded every second for approximately 3 minutes. A data set was obtained at each N/N_{js}. The arithmetic mean of each data set was noted. This procedure was repeated twice for each N/N_{js}. The arithmetic mean of these two results was reported. Power consumption was calculated using Equation (3) in Chapter 1. All experiments were performed at N_{js}.

CHAPTER 4

RESULTS AND DISCUSSION

4.1 Clarification of the Definition of Cloud Height

Current definition of cloud height in literature has some unclear points that cause inconsistencies between different studies. Measurement point of cloud height and parameters of solids concentration and impeller speed that are known to affect cloud height does not take place in the current definition. In order to enlighten these unclear points about cloud height, three key issues were identified. These issues are determination of possible measurement points, identification of the most meaningful measurement point and identification of limitations on impeller speed and solids concentration for a meaningful cloud height definition. The findings of these key issues are given in this order in the following sub-sections. Based on these findings, a clear definition of cloud height is proposed.

4.1.1 Determination of Measurement Point of Cloud Height

Measurement of cloud height is not straightforward due to its fluctuating nature as mentioned in Chapter 1. Therefore, first, possible measurement points of cloud height were identified, then the measurement point of cloud height was determined.

4.1.1.1 Determination of Possible Measurement Points

A significant variation in the height of solids cloud was observed across the cross section of the tank. This variation is shown in Figure 4.1. The first step in determining possible measurement points was to divide the cross section of the tank into regions. The cross-section of the tank was divided into three regions: front of

the baffle, mid-baffle, and back of the baffle, as shown in Figure 4.1. The observations showed that these three regions give different cloud height values. The height of the solids cloud is the maximum in front of the baffle. It declines towards the back of the baffle. It should be noted that this decline was observed for a PBT impeller; for another type of impeller a different analysis may be needed.

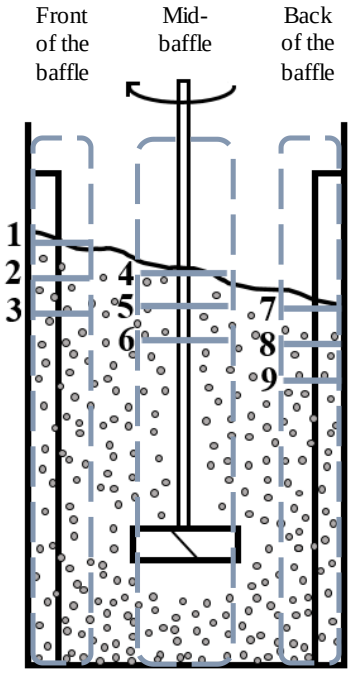

Figure 4.1. Possible measurement points and the corresponding regions

In each region shown in Figure 4.1, solid cloud appears at three different levels during mixing. Based on this observation, nine possible cloud height measurement points were identified. Nine possible measurement points between two baffles represented with points 1 to 9 in Figure 4.1.

Consider the three possible measurement points identified in the front of the baffle region. Point 1 corresponds to the maximum height that the solids can reach. It should be noted that this is the maximum height that the solids reach as a whole. The occasional bursts of only a few solid particles, which can reach a higher level than

point 1 were not considered here. Point 2 corresponds to the average height of the solids cloud during mixing. Point 3 corresponds to the minimum height that the solids cloud reach. This maximum, average and the minimum solid cloud heights are seen in each of the three regions. Throughout the tank, the maximum point that the solids reach is point 1 and the minimum point that the solids reach is point 9. There is no clear information about which point reported cloud height data in majority of the studies in literature. Only a limited number of studies reported the measurement point. All the measurement points reported in these studies were not clear. One cannot confidently say which point was reported as cloud height data in these studies, but one can say that different studies reported cloud height data that is obtained from different regions shown in Figure 4.1. While there is no clear information about which point was used to record cloud height data, it is suspected that readings from point 5 were reported in the majority of literature.

The importance of identifying a certain measurement point for cloud height can be shown by an analysis of deviation between measurements obtained from different points. For this analysis, 6 vol% slurries of SG, MG, LG, BG and Garnet were tested at N_{js}. Three measurement points were selected out of nine possible measurement points for comparison: point 1 which gives the maximum height solids can reach across the tank, point 5 which is the average cloud height in the mid-baffle plane and point 9 which gives the minimum height solids reach across the tank. The data is given in Figure 4.2.

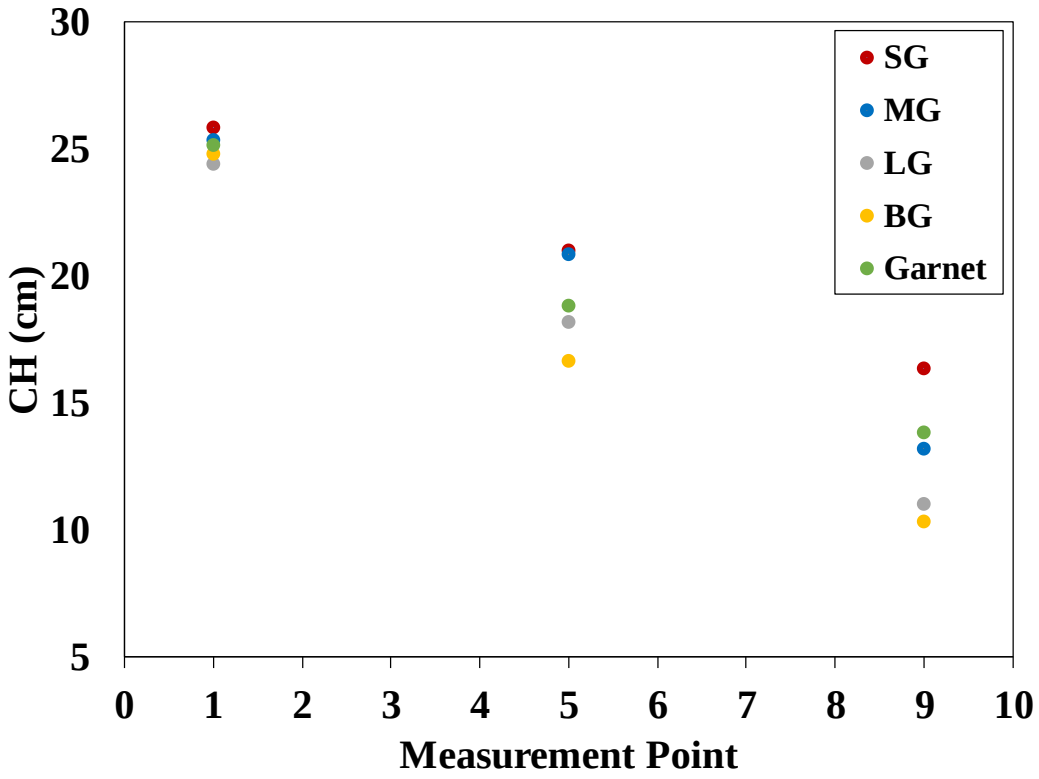

Figure 4.2. Comparison of cloud height measurements at three measurement points for five particle types at 6 vol%

A remarkable variation in cloud height between point 1 and 9 can be clearly seen in Figure 4.2. For all particles, cloud height is much lower at point 9. Another important observation from this figure is the variation of cloud height data due to varying physical properties of the particle at each measurement point. At point 1, all particles result the almost same cloud height data whereas at point 5 and 9, cloud height varies as particle properties vary. At point 5, SG and MG result almost the same cloud height data, but cloud height considerably decreases as particle size increases beyond MG. Additionally, a decrease in cloud height is observed as density of the particle increases. At point 9, the difference becomes significant as the particle size increases from SG to BG, although the density of the particle does not seem very effective on cloud height at this point.

The variations of data observed at point 1 and 9 are evaluated with respect to the data observed at point 5. The percent differences between points 5 and 1 and points 5 and 9 are given for all particle types in Table 4.1.

Table 4.1 The percent differences of cloud height data at the average point (point 5) from the maximum and minimum points

Particle Name	% difference between points 5 and 1*	% difference between points 5 and 9
SG	23.0	22.2
MG	21.6	36.8
LG	34.4	39.4
BG	49.0	38.0
Garnet	33.6	26.5

*Absolute values are given.

The variations between points 5 and 1 and points 5 and 9 are resulted quite large for all particles. Minimum and maximum percent variations are ~22% and 49%, respectively. The maximum variation of point 1 from point 5 was obtained with BG as 49% whereas the maximum variation of point 9 from point 5 was obtained with LG as ~39%. These observations show that the data taken at different parts of the tank can be very different, and almost impossible to compare. This highlights the importance of identification of the most meaningful point for the measurement of cloud height and proposing gathering the developing literature towards measurements in a single location that is comparable and repeatable.

4.1.1.2 Identification of The Most Meaningful Measurement Point

In this section, the nine possible measurement points that were determined in the previous section are analyzed to identify the most meaningful measurement point. Experiments were performed using red food dye. Dye experiments were used by Brown (2018) to identify poor mixing region above the cloud. A similar method was applied here to identify the best measurement point. Dye formed a contrast in the tank. This contrast helped to visually observe the bulk motion of solids and the interface between solid-rich and liquid-rich volumes.

In this analysis, there were two systems to be investigated: a single-phase and a slurry system. Single-phase system consisted of only water whereas slurry system consisted of 6 vol% slurry of MG. Both systems were operated at an impeller speed equal to N_{js} of the slurry system. The dye feed points for both systems were the same. Feed points for both systems are shown in Figure 4.3a and b. This point corresponds to a level that is higher than the top of the impeller. It is in front of the baffle and very close to the tank wall. The experiments were conducted in a tall tank (H=1.5T).

Figure 4.3a shows how mixing evolved in the single-phase system. The dye allowed tracking the flow pattern. The dye went up along the front of the baffle right after the injection. Then, it went down through the middle region of the tank by the suction of the impeller. Owing to the loop that the impeller formed, the injected dye was completely blended in 7 seconds.

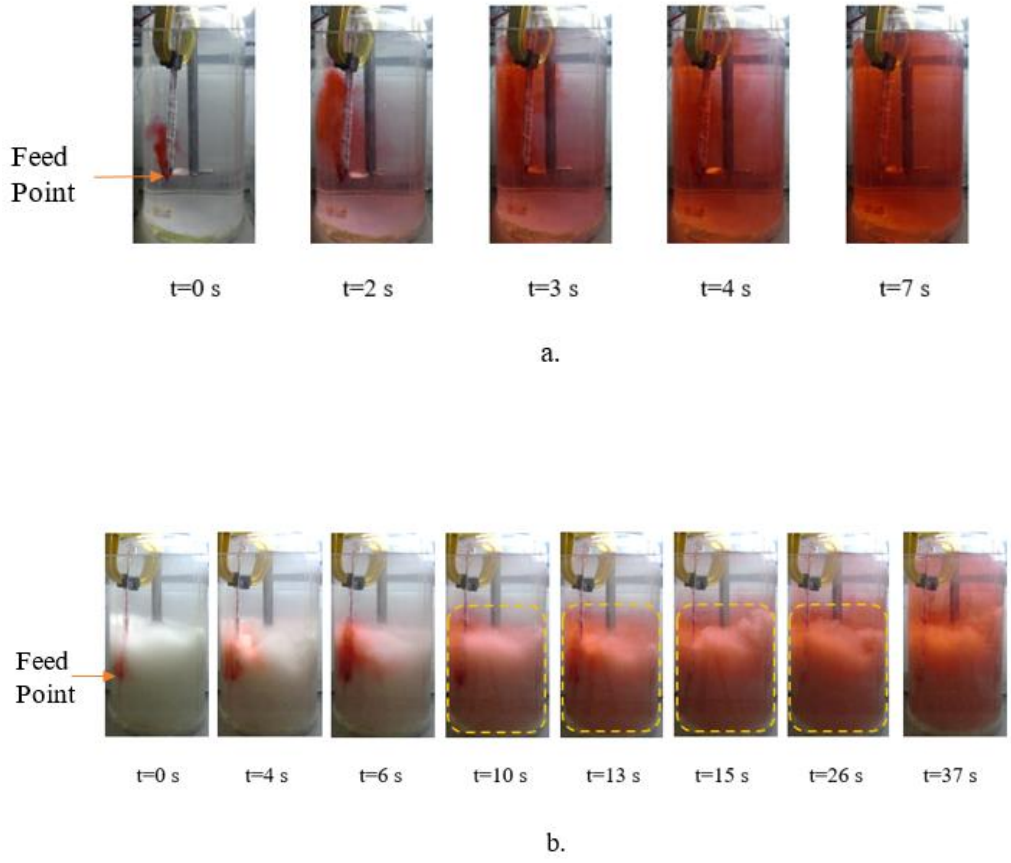

Figure 4.3. Dye experiments in (a) single-phase system and (b) slurry system

The feed point of the dye was within the solid cloud in the slurry system as shown in Figure 4.3b. For the first 4 seconds, the dye blended only in the cloud. The region above cloud remained clear. The first color change in the region above the cloud occurred at the 6th second. The dye protruded to the liquid-rich volume as a result of the bursts of the solid cloud. The point that the dye reached in the liquid-rich volume was the maximum point that bulk of the solids can reach. This point corresponds to point 1 in Figure 4.1. At t=10 s, a layer of dye that has a height that is equal to point 1 appears within the liquid-rich volume. This dye layer remained at this location up to 26th second without blending thoroughly. It should be noted that the dye was continuously fed to the tank; therefore, colour throughout gets darker over time as can be seen in Figure 4.3b. Diffusion of the dye also takes place. In Figure 4.3b, at

the 26th second, the height of the dye layer seems to increase; however, this so-called increase is mainly due to diffusion of the dye. The actual height of the dye layer is related to the maximum point that solids can reach in the front of the baffle. The height of the dye layer that remained almost constant for a substantial time began appearing with the motion of particles; therefore, it represents the height of the volume that the particles actively used. This height, which is also equal to the maximum height that solids can reach, can be expressed as cloud height. Beyond this point, no particle existed except for very rare bursts of only a few particles. The dye did not blend throughout the tank for a very long time, until the 37th second, which indicated very poor mixing above the cloud height.

This finding is in line with a recent study that investigated the turbulence decay above the solids cloud (Ayranci & Kresta, 2021). They found that turbulence decays until the maximum point at which cloud height is measured, and beyond this point, turbulence remains constant at a value near zero.

Selecting the maximum point that the bulk of solids can reach as the cloud height presents a very practical advantage. Determination of the maximum point that the bulk of the solids can reach is much simpler in terms of observation, highly repeatable both for a single observer and among different observers. It is easier to visualize 'the maximum height that solids can reach' than 'the height to which solids are suspended,' which is very general and ambiguous.

The errors between three measurements by the same observer at the three measurement points are given in Table 4.2. These errors belong to the data set given in Figure 4.2. The error is the maximum at point 9 and the minimum at point 1. By setting the measurement point to the maximum point that the solids can reach as a bulk it is possible to obtain highly reproducible data. Based on this analysis and the results of the dye tests it is recommended to measure and report the cloud height as the maximum point that the solids can reach.

Table 4.2 The maximum error (%) between three cloud height data taken at different times at measurement points of 1, 5 and 9

	Measurement Point		
	1	5	9
SG	1.0	4.7	3.0
MG	2.0	7.0	3.7
LG	1.0	2.7	9.1
BG	3.9	5.9	9.1
Al_2O_3	2.0	5.0	7.1
Garnet	2.0	2.6	3.4

A set of experiments were performed in an H=T tank. Slurries of MG particles at solids concentrations varying between 9 - 25 vol% when off-bottom clearance was equal to T/3. Besides, a couple of experiments were also performed for off-bottom clearance values of T/6 and T/4 with 5 vol% MG slurry. All tests were performed at N_{js}.

Based on the determined measurement point, point 1, no cloud height data could be recorded as no interface existed throughout the tank in which the off-bottom clearance was T/3. The solids reached the liquid surface and were distributed throughout the tank. This result showed that solids could use all of the volume in a tank in which the liquid height is equal to the tank diameter, at N_{js}. This finding was tested using particles that have significantly larger densities –Garnet and Steel–, and the same result was obtained.

In the tests performed with 5 vol% MG slurry at off-bottom clearance of T/4, all solids reached to liquid height and were distributed throughout the tank as well. However, in the tests performed at off-bottom clearance of T/6, an interface was observed. As the off-bottom clearance is decreased the interaction between the impeller and solids at the bottom is improved. Thus, less energy is required to lift

solids from the bottom. That is, the degree of complete suspension is reached at a lower impeller speed. Nevertheless, at the degree of complete off-bottom suspension, the energy supplied from an impeller located at a lower position cannot enable the solids to reach a level that solids can reach using an impeller located at a higher position. This may be the reason behind that an interface was observed at off-bottom clearance of T/6.

The majority of the experiments in this study was planned to be carried out at N_{js} and off-bottom clearance of T/3. At these conditions, the solids were distributed throughout an H=T tank as mentioned above. This causes the observations of cloud height to be more challenging, even sometimes impossible. In the rest of the experiments performed in the scope of this study, liquid height was set at 1.5T due to the clarity and the convenience of cloud height observations.

4.1.2 Identification of Limitations and Effects of Solids Concentration and Impeller Speed on Cloud Height

Solids concentration and impeller speed have significant effects on cloud height that cannot be neglected. Nonetheless, the current definition of cloud height in literature is deficient in terms of these two important parameters. To eliminate the deficiencies in the current cloud height definition, the effects of solids concentration and impeller speed on cloud height were investigated. Based on the findings, limitations of solids concentration and impeller speed on cloud height were identified. MG was used as the main particle in these experiments; LG and Garnet were used to test the limits identified by using MG.

4.1.2.1 Identification of Limitations and Effects of Solids Concentration on Cloud Height

Slurries of MG at varying solids concentration between 0.5–25 vol% were used. The experiments were performed at N_{js}. Each experiment was recorded on the video. The

snapshots of each experiment are shown in Figure 4.4. In figure, levels of liquid height and cloud height are indicated by blue and red lines, respectively. These indicators were used to develop a better understanding of the results because the camera distorted the actual views of the equipment, including the sizes and the positions. The level of the red line, i.e. the actual level that cloud height data was recorded, was determined proportioning the tank size in the images to the actual size of the tank.

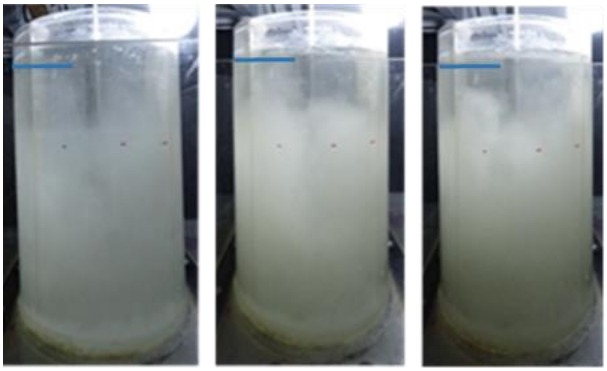

a. Part I: 0.5-1.5 vol%

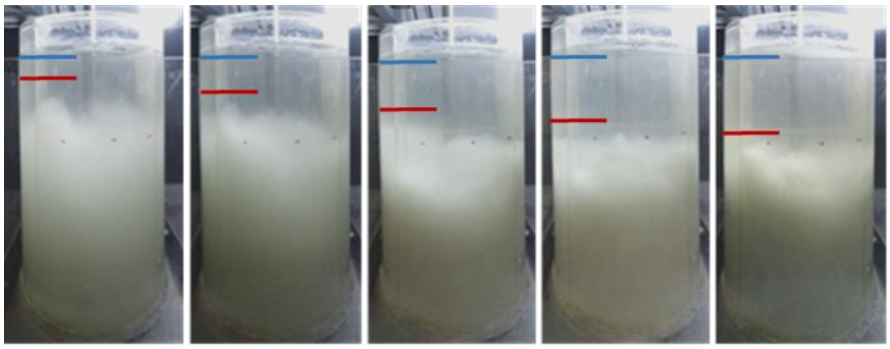

b. Part II: 2-7 vol%

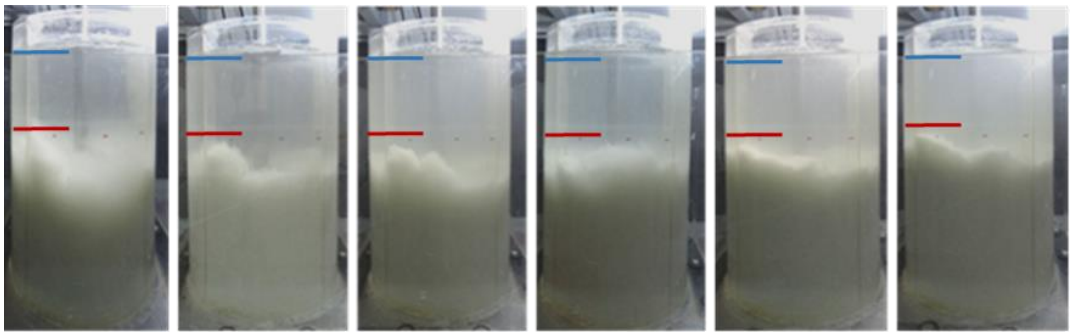

c. Part III: 9-25 vol%

Figure 4.4. Variation of solids height with increasing solids concentration (a) Part I: 0.5-1.5 vol% (b) Part II: 2-7 vol% (c)Part III: 9-25 vol%

At very low solids concentrations, almost all of the particles were lifted up to the liquid surface. As concentration was increased, the amount of the particles that were lifted up to the liquid surface decreased. As solids concentration was increased, power supplied by the impeller into the system was shared by a greater number of solid particles to be suspended. Therefore, the maximum height that solids can reach reduced. As shown in Figure 4.4a, there was no clear interface between solid-rich and liquid-rich parts of the tank until 1.5 vol% since solids were distributed throughout the tank. This means that a meaningful cloud height cannot be recorded up to 1.5 vol%**.** Figure 4.5 shows cloud height data of the snapshots given in Figure 4.4. There is no cloud height data in Part I of Figure 4.5, since a meaningful cloud height could not be observed in the range of 0.5-1.5 vol%.

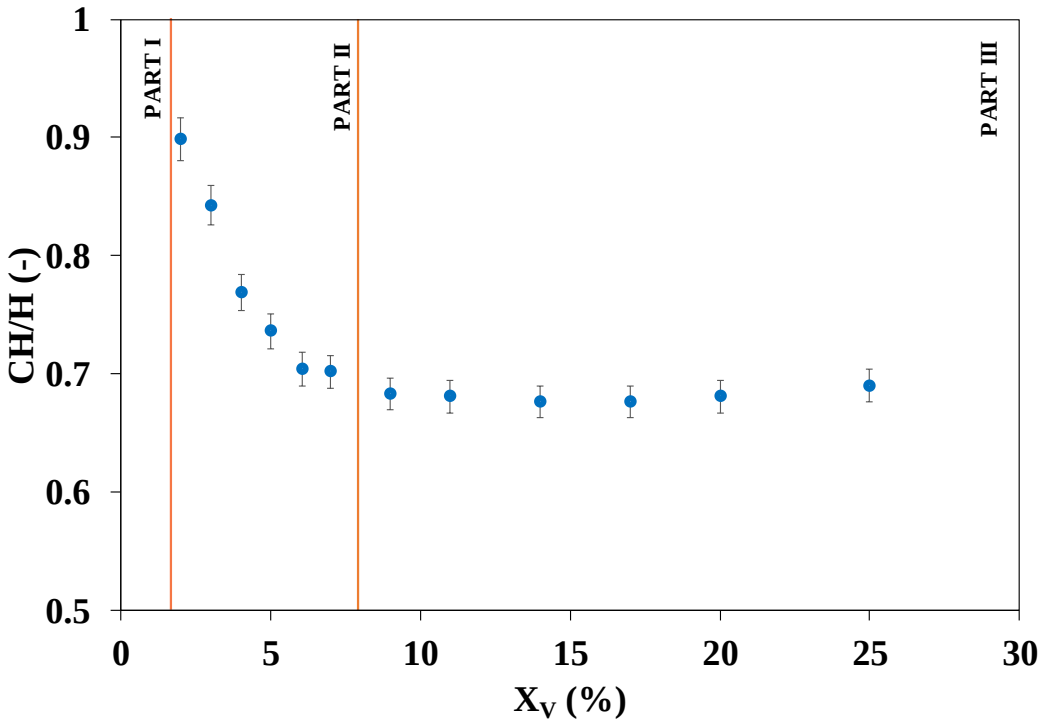

Figure 4.5. Variation of cloud height relative to the liquid height with increasing solids concentration. Part I, Part II and Part III correspond to the solids concentration ranges given in Figure 4.4.

At 2 vol%, for the first time, an interface was observed between liquid-rich and solid-rich parts of the tank. This means that a meaningful cloud height data can be recorded at and above 2 vol%. This gives a lower limit on the definition of cloud height. When solids concentration was increased from 2 to 7 vol%, a decreasing trend in cloud height was observed as shown in Figure 4.4b**.** The corresponding data is given in Figure 4.5 as Part II. When a power law fit was applied to the data in Part II, it was found that cloud height is proportional to $X_V^{-0.213}$.

In the last part, when solids concentration was increased from 9 vol% to 25 vol%, cloud height almost did not change with increasing solids concentration. It can be seen in both Figure 4.4c and Part III of Figure 4.5. The difference between the maximum and the minimum cloud height data in this range was found as 2%, proving

that almost no change in cloud height occurred while solids concentration was increased between 9 and 25 vol%. It can be concluded that a persistent cloud height was achieved above 9 vol %. It should be noted that the exponent of -0.213 in Part II is only valid for MG. This exponent may vary depending on the type of the particle.

To test the validity of the limits on concentration identified by MG slurries, a particle with different size but the same density –LG– and a particle with different density but similar size –Garnet– were used. The solids concentration of slurries with these particles was varied between 0.5 vol% to 20 vol% at N_{js} of corresponding particle. Cloud height data of MG, LG and Garnet were compared in Figure 4.6. As seen in this figure, cloud height data of LG and Garnet begins from 2 vol%. The reason is that a meaningful cloud height could be observed beginning form 2 vol% for both particle types. This shows that the minimum concentration limit which was determined with MG slurries also applies to LG and Garnet.

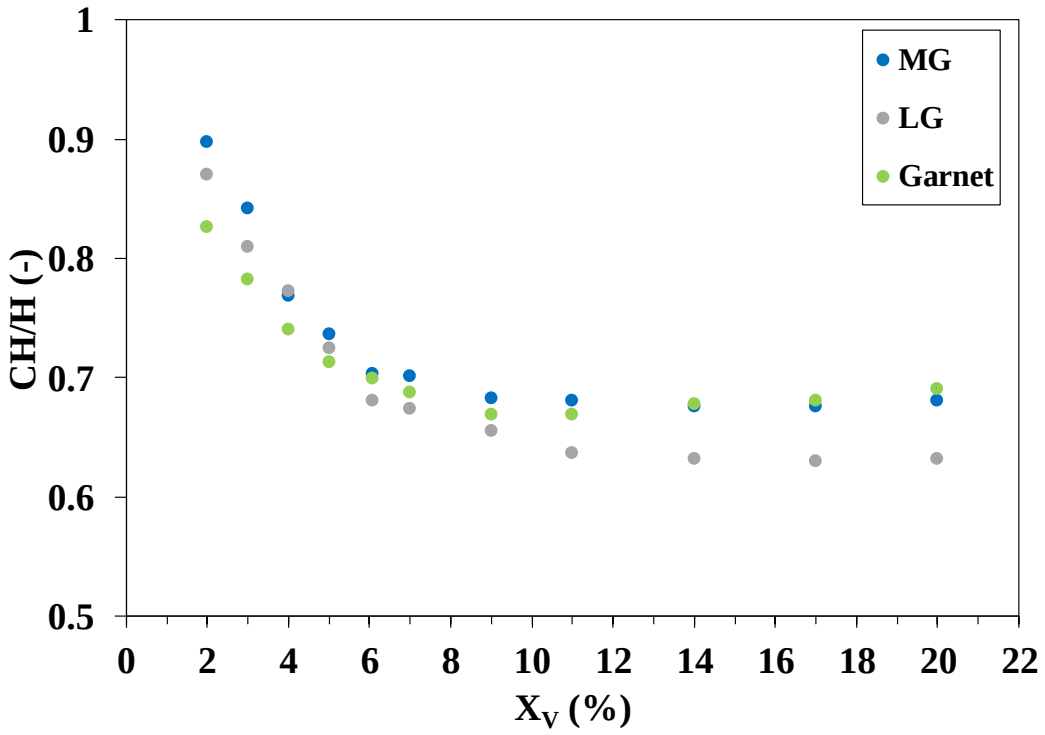

Figure 4.6. Variation of cloud height relative to the liquid height with increasing solids concentration for MG, LG and Garnet

The change in cloud height data of Garnet with increasing solids concentration between 2 and 20 vol% was less than the change in cloud height data of particles that had lower density. According to this, cloud height of a particle that has a higher density does not change as much as a particle that has a lower density along increasing solids concentration. Cloud height data of Garnet was lower compared to MG and LG between 2-4 vol%. However, beginning from 6 vol%, cloud height data of Garnet and MG were almost the same, while cloud height data of LG appeared like an outlier.

Between 2-7 vol%, cloud height decreased due to increasing solids concentration for both LG and Garnet. For LG this decrease can be represented with an exponent of -0.215, and for Garnet it can be represented with an exponent of -0.152. As it can be seen in Figure 4.6, the most drastic decrease of cloud height in this concentration range was observed for MG among three particle types. It can be concluded that cloud height decreases between 2-7 vol% more mildly as the size or the density of the particle is increased.

Between 9-20 vol%, as solids concentration was increased cloud height data of LG slightly decreased whereas cloud height data of Garnet slightly increased. The difference between the maximum and the minimum data in this concentration range is 3.9% and 3.2% for LG and Garnet, respectively. It can be assumed that the cloud height data of LG and Garnet almost did not change with increasing solids concentration above 9 vol%. This is in line with the findings of the investigation carried out using MG slurries.

In the studies in literature solids concentration was expressed in terms of both weight percent and volume percent, while in general weight percent was preferred. In determining limits of solids concentration for a meaningful cloud height data that is applicable to all types of solids, one should be careful about how to express solids concentration. The preliminary studies of this work showed that at a fixed weight

percent, the limits on solids concentration identified above change from one type of particle to another. This is because, at the same weight percent, the number of particles with different densities, such as MG (2500 kg/m^3) and steel (7595 kg/m^3), are very different from each other. On the other hand, when volume percent is used, the limits identified above are all the same for different types of particles. This is why volume percent was used in expressing solids concentration in this study, and it is recommended to be used in investigating the relation between cloud height and solids concentration.

4.1.2.2 Identification of Limitations and Effects of Impeller Speed

Preliminary experiments indicated that there was no clear interface between liquid-rich and solid-rich parts of the tank at low impeller speeds. Bujalski et al. (1999) reported that at low impeller speeds small portion of the particles were suspended and no clear interface was observed. Based on findings of this study and some studies in literature, a lower limit on impeller speed should be identified in order to observe a meaningful cloud height. In the analysis of the change in cloud height with increasing impeller speed, an MG slurry of 6 vol% was used. Lower limit on impeller speed that is determined using MG was tested with 6 vol% slurries of LG and Garnet. Solids concentration of the slurries used in this analysis is within the range where a meaningful cloud height can be determined based on the findings explained in the previous part. The experiments were recorded on a video. The snapshots of the video for each part of this analysis are shown in Figure 4.7. Similar to Figure 4.4, the liquid level and the cloud height are indicated with a blue line and a red line, respectively.

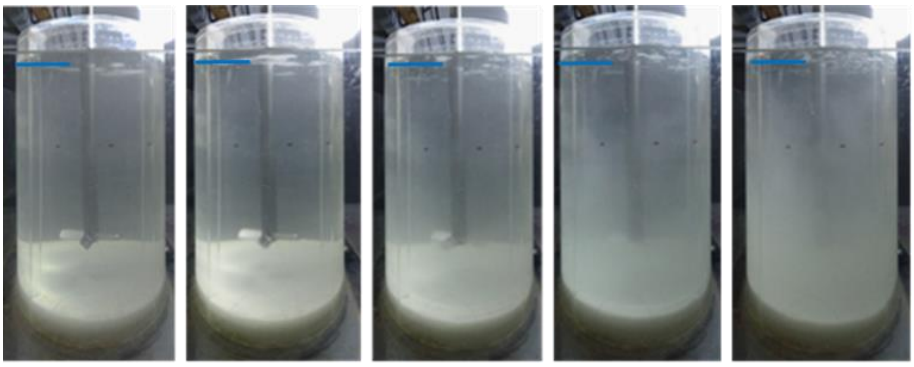

a. Part I: 0.06 – 0.29 N_{js}

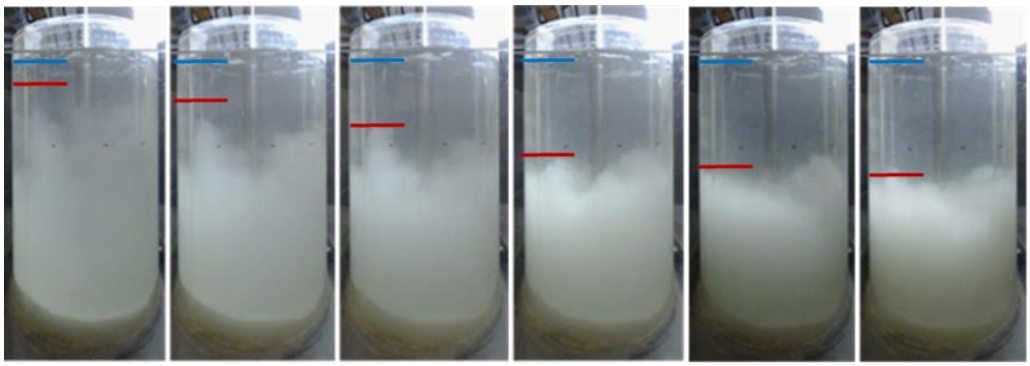

b. Part II: 0.32-0.48 N_{js}

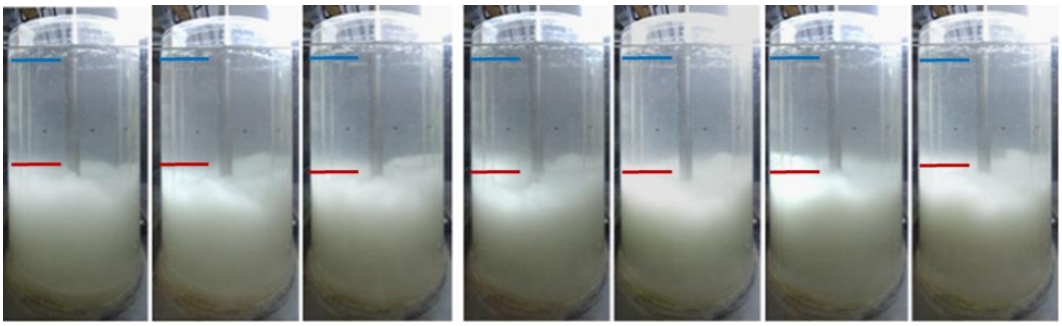

c. Part III: 0.52-0.71 N_{js}

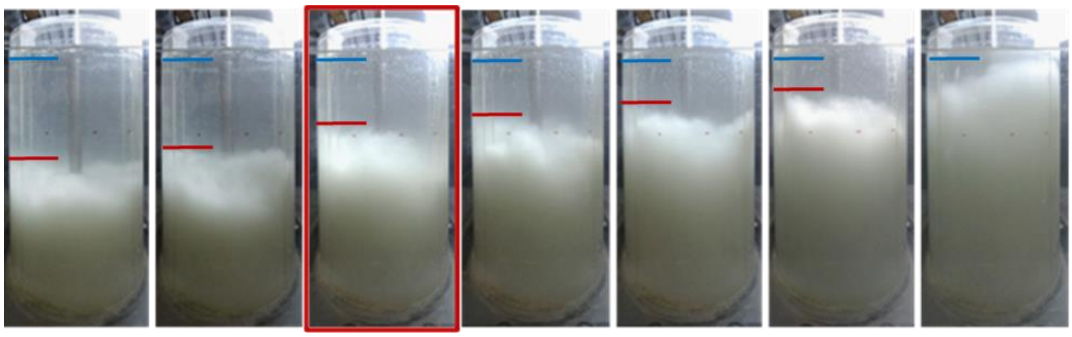

d. Part IV: 0.75-1.45 N_{js}

Figure 4.7. Variation of solids height with increasing impeller speed (a) Part I: 0.06-0.29 N_{js} (b) Part II: 0.32-0.48 N_{js} (c) Part III: 0.52-0.71 N_{js} (d) Part IV: 0.75-1.45 N_{js}

Most of the solid-liquid mixing processes in industry operate at complete off-bottom suspension conditions. The corresponding impeller speed at this condition is the just suspended speed, N_{js}. A cloud height definition must involve impeller speed, and for a solid-liquid mixing operation impeller speed should be in terms of this key design parameter, N_{js}. Expressing impeller speed in terms of N_{js} provides comparability among different types of particles as being at the same solids suspension degree. In this study; therefore, the impeller speed values are reported in terms of N_{js}.

In this analysis, the impeller speed was varied between $N=0.06N_{js}$ and $N=1.45N_{js}$ with 25 rpm increments. As shown in Figure 4.7a, no clear interface was observed until $N=0.29N_{js}$. The non-existence of a clear interface occurs in different forms within this impeller speed range. At very low impeller speeds, no particles were suspended. As impeller speed was increased, very little portion of particles were suspended suddenly up to the height that equals to the liquid height. Further increase in impeller speed caused particles to be suspended in larger amounts and the height to which solids were suspended to be decreased. This was simply because a much higher number of particles shared the energy supplied by the impeller. Under these conditions some small portion of particles reach the liquid surface, a portion of the

particles remain above the solid bed, but a cloud cannot be observed, so as a clear interface. It should also be noted that in this impeller speed range a solid bed always exists. The results of the investigation on cloud height change due to increasing impeller speed is given in Figure 4.8. There is no cloud height data takes place in Part I of Figure 4.8 since no interface formed between $N=0.06N_{js}$ and $N=0.29N_{js}$.

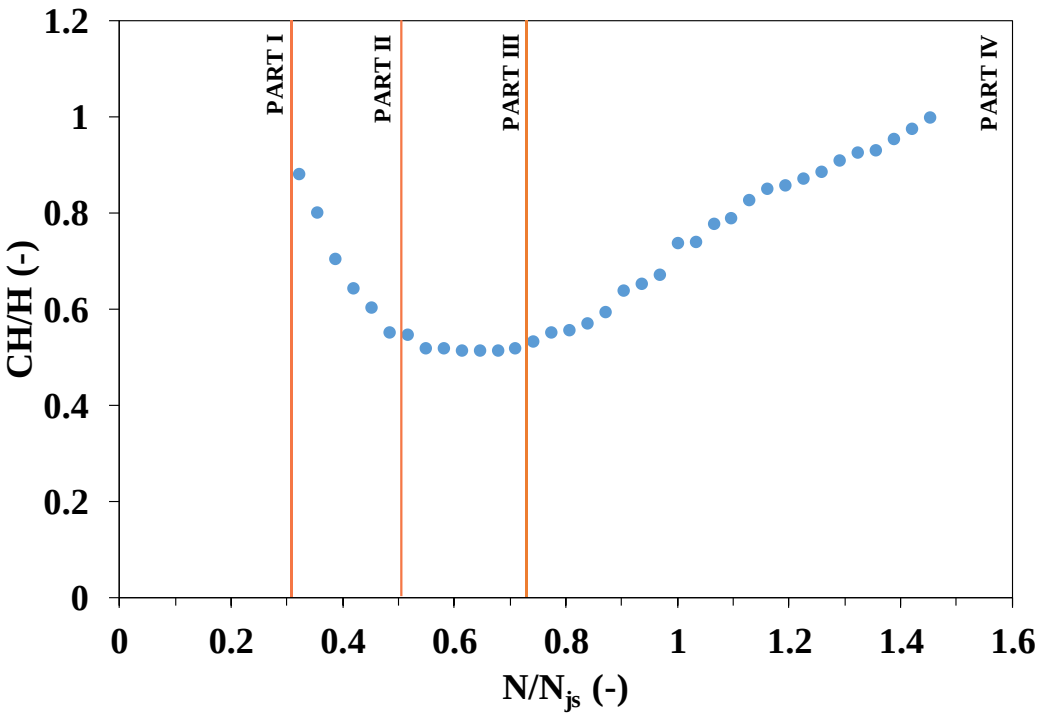

Figure 4.8. Variation of solids height relative to the liquid height with increasing impeller speed. Part I, Part II, Part III and Part IV correspond to the impeller speed ranges given in Figure 4.7

When impeller speed was increased to and above $N=0.32N_{js}$ a cloud height began to appear. This shows that a meaningful cloud height can be recorded beginning from impeller speed equal to $0.32N_{js}$. Between $N=0.32N_{js}$ to $N=0.48N_{js}$, a decreasing trend in cloud height was observed, as shown in Figure 4.7b. For this impeller speed range, which is indicated as Part II in Figure 4.8, the decrease of cloud height is proportional

to $(N/N_{js})^{-1.16}$. The solid bed at the bottom of the tank was still quite visible within Part II.

Almost no change in cloud height with increasing impeller speed between $N=0.52N_{js}$ to $N=0.71N_{js}$ was observed as shown in both Figure 4.7c and Part III in Figure 4.8. The reason for no change in cloud height may be that energy supplied from the impeller within this impeller speed range was mostly spent by the stationary solids to be suspended. The difference between the maximum and the minimum data in this impeller speed range is 5%, proving cloud height was not significantly affected by the increase in impeller speed between $N=0.52N_{js}$ and $N=0.71N_{js}$. In this part, the solid bed at the bottom of the tank was still visible.

In the last part, the impeller speed was increased from $N=0.75N_{js}$ to $N=1.45N_{js}$. In Figure 4.7d, the image which is indicated with a red box corresponds to $N=N_{js}$. Cloud height linearly increased with a slope of 0.69 as impeller speed was increased. This linear increase can be seen in Figure 4.7d and Part IV of Figure 4.8. At the beginning of Part IV, the solid bed disappeared. The linear increase along this part might be due to the loss of solid bed. When impeller speed was increased to $N=1.45N_{js}$, solid cloud covered all of the tank volume, such that no interface was observed at this impeller speed. The analysis of the limitations on impeller speed indicated that a meaningful cloud height could be observed at impeller speeds between $N=0.32N_{js}$ and $N=1.45N_{js}$. It should be noted that the upper limit of $N=1.45N_{js}$ is valid for a system in which H=1.5T; this limit is expected to change as the liquid height is changed.

In order to test the validation of the limits on impeller speed identified by MG slurry, slurries of a particle with different size but the same density –LG– and a particle with different density but a similar size –Garnet– were examined from $N=0.08N_{js}$ to $N=1.49N_{js}$. These tests were performed using 6 vol% slurries. Cloud height data of MG, LG and Garnet were compared in Figure 4.9.

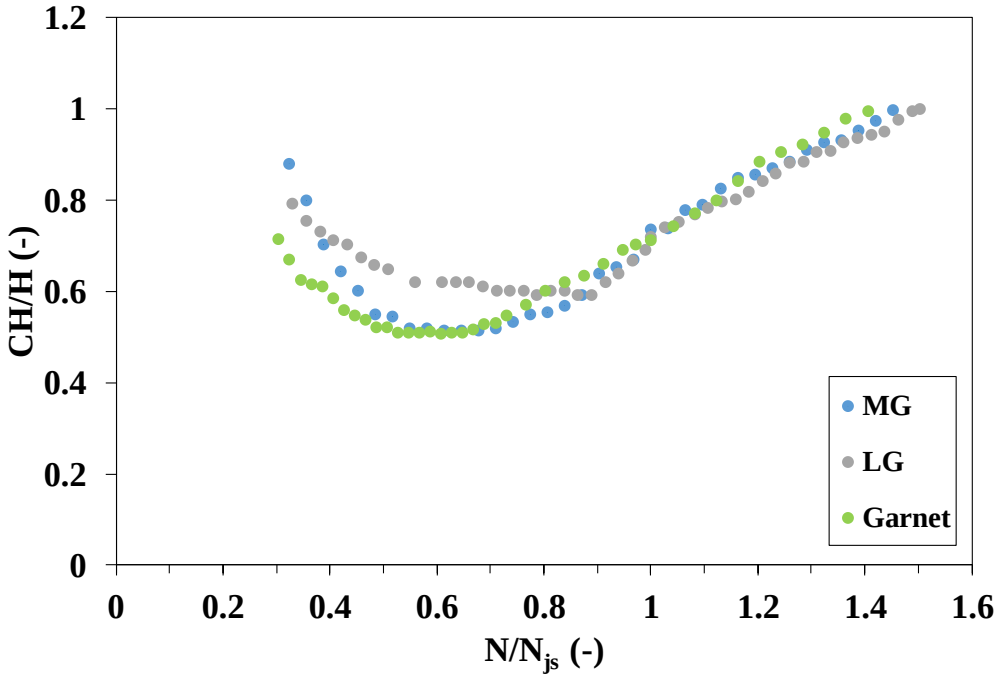

Figure 4.9. Variation of solids height relative to the liquid height with increasing impeller speed for MG, LG and Garnet

The lower limit on impeller speed to observe a meaningful cloud height formation was found as $N=0.33N_{js}$ and $N=0.30N_{js}$ for LG and Garnet, respectively. Cloud height data of LG decreased with increasing impeller speed between $N=0.33N_{js}$ and $N=0.51N_{js}$. For LG this decrease can be represented with an exponent of -0.45. As seen in Figure 4.9, similar to LG a decreasing trend of cloud height was observed also for Garnet but within the range of $N=0.30N_{js}$ to $N=0.47N_{js}$. For Garnet this decrease can be represented with an exponent of -0.63. Similar decreasing profile was observed with MG as indicated as Part II in Figure 4.8. The most drastic decrease of cloud height due to increasing impeller speed was observed for MG. It can be concluded that cloud height changes more mildly with increasing impeller speed as the size and the density of the particle is increased.

Cloud height stayed almost constant as the impeller speed was increased between $N=0.56N_{js}$ and $N=0.86N_{js}$ for LG, and between $N=0.49N_{js}$ and $N=0.65N_{js}$ for Garnet.

This can be seen in Figure 4.9. The difference between the maximum and the minimum data within these impeller speed ranges are 2.2% and 4.5% for LG and Garnet, respectively.

For LG cloud height linearly increased due to increasing impeller speed after $N=0.89N_{js}$ with a slope of 0.61. At $N=1.49N_{js}$, solids were distributed throughout the tank and the interface disappeared. Similar to MG and LG, cloud height data of Garnet linearly increased within the last part of this analysis. An increase in cloud height was observed with a slope of 0.67 until $N=1.40N_{js}$. Solids cloud were distributed throughout the tank at $N=1.40N_{js}$.

The limitations on impeller speed determined using LG and Garnet slurries are in line with the limits identified using MG slurry. Arithmetic mean of lower and upper limits on impeller speed to observe a meaningful cloud height determined with MG, LG and Garnet was found as $N=0.32N_{js}$ and $N=1.45N_{js}$, respectively.

The studies that investigated the effect of impeller speed on cloud height observed two different types of behavior: increasing cloud height with increasing impeller speed (monotonic) or irregular trend in cloud height with increasing impeller speed (non-monotonic). In this study, a non-monotonic behavior of cloud height with increasing impeller speed within the lower and upper limits of impeller speed was observed.

4.1.3 Detailed Definition of Cloud Height

The deficiencies in the current definition of cloud height were identified as a clearly defined measurement point and limitations on impeller speed and solids concentration. The findings of the determination of possible measurement points, identification of the most meaningful measurement point and identification of limitations on solids concentration and impeller speed allowed developing a detailed definition of cloud height.

The definition must include the measurement point. The cloud height should be measured at the maximum point that bulk of the solid particles can reach across the cross section of the tank. The definition should involve the parameters of solids concentration and impeller speed. In general, cloud height is known as the height of a fluctuating interface between the solids-rich and liquid-rich parts of the tank. However, this interface cannot be observed at low solids concentrations and low and very high impeller speeds. Thus, lower and/or higher limits on solids concentration and impeller speed are required to measure a meaningful cloud height data. In expressing solids concentration, volume percent should be used in order to generalize the definition of the cloud height for all types of particles.

Based on these, a detailed and clarified definition of cloud height is proposed as the following:

> Cloud height can be measured only when an interface forms between the solid-rich and liquid-rich parts of the tank. The height of this interface should be measured at the maximum height that solids can reach, which is the in front of the baffle for the configuration used in in this study. Cloud height occurs at and above an impeller speed of $N=0.32N_{js}$ and at and above a solids concentration of 2 vol%. A persistent cloud height is achieved above 9 vol%. The cloud height disappears beginning from $N=1.45N_{js}$ for a tank with H=1.5T, as the solids are distributed throughout the tank.

4.2 Effects of Solids Concentration, Impeller Speed, Particle Properties and Off-Bottom Clearance on Cloud Height

The analysis up to here showed that the solids concentration and impeller speed are parameters that influence cloud height. The analyses in the previous sections were performed with the aim of finding the limits of a clear definition of cloud height. In the following two parts, the analysis is done to investigate the effects of these

parameters on cloud height in more detail with a final goal of obtaining a correlation to predict the cloud height. Particles that have the same densities but different sizes and that have similar sizes but different densities were tested. In this section, the effects of particle properties and off-bottom clearance on cloud height are also investigated. In the analysis presented in the following subsections, slurries of SG, MG, LG, BG, Al_2O_3 and Garnet were used. Except for the investigation given in Section 4.2.2, in which the effect of impeller speed is discussed, all experiments presented were carried out at N_{js}.

4.2.1 Effect of Solids Concentration on Cloud Height

In the previous part, the effect of solids concentration on cloud height was discussed based on the results of the investigation conducted using slurries of MG, LG and Garnet at N_{js}. In this part, analysis of the effect of solids concentration on cloud height was performed using slurries of SG, MG, LG, BG, Al_2O_3 and Garnet at N_{js}. Cloud height data of SG, MG, LG and BG for increasing solids concentrations are shown in Figure 4.10.

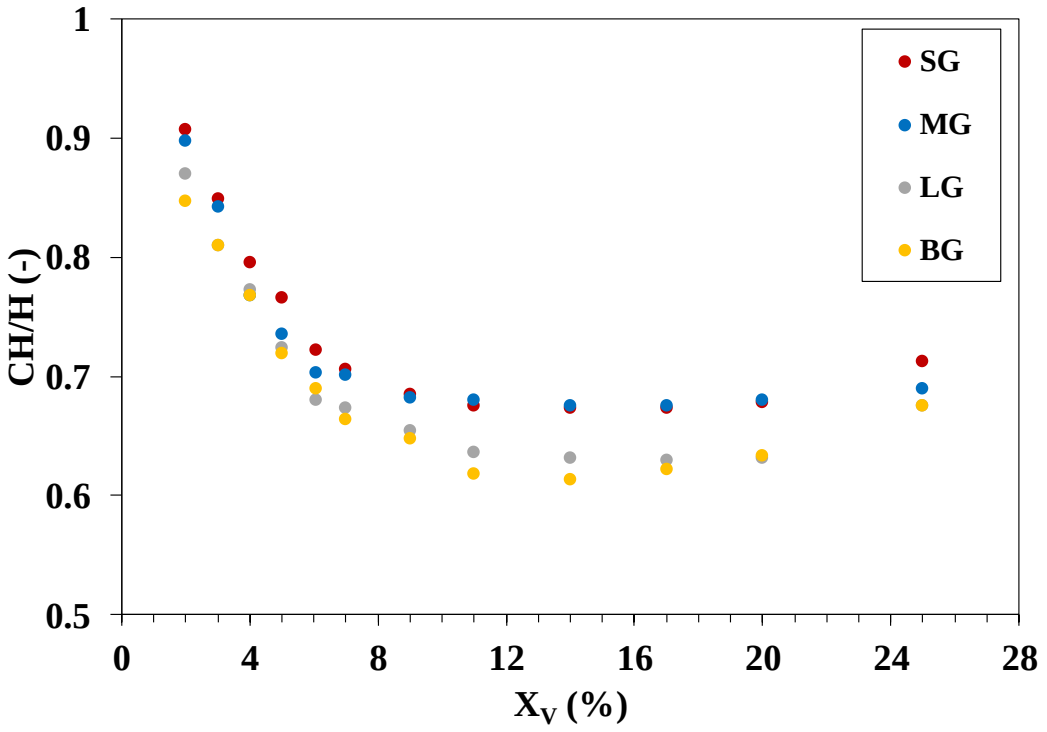

Figure 4.10. Variation of cloud height relative to the liquid height with increasing solids concentration for SG, MG, LG and BG

For all particles, a decrease in cloud height due to increasing solids concentration between 2 and 9 vol% was observed. The cloud height remained the same between 9 and 20 vol% for SG, MG and LG slurries, which then increased at the highest concentration of 25 vol%. For the BG slurry, the increasing trend began at a lower concentration of 17 vol%.

A sharp decrease in cloud height data of all particles with increasing solids concentration between 2 and 7 vol% was observed. This decrease in cloud height can be represented with the exponents given in Table 4.3. As the size of the particle is increased from SG to LG, which is from 124 to 574 µm, the slope of the decrease increases. The largest particle, BG, changes this trend as it gives an exponent the same as SG. The values given in Table 4.3 are still similar to each other.

Table 4.3 The exponents on X_V for particles that have different sizes between solids concentration of 2 and 7 vol%.

	Exponent on X_V
SG	-0.205
MG	-0.213
LG	-0.215
BG	-0.206

The reason of the decrease in cloud height until 9 vol% may be because the energy supplied by the impeller is shared by a greater number of particles as solids concentration is increased After a threshold value of 9 vol%, however, the particle-particle interactions begin to be significant. This helps suspension of particles, which do not allow further decrease of the cloud height. Above 20 vol%, possibly another threshold value is seen where the increased number of particles, and therefore number of collisions allow for the particles to move further up in the tank. It should be reminded that the cloud height data is taken at N_{js} of each slurry. This means that the impeller speed in Figure 4.10 increases as the solids concentration is increased. It is possible that the increase in the impeller speed is more pronounced at the highest concentration. This increase is needed for the suspension of the particles at the bottom of the tank, but for the already suspended particles this means a significantly a greater number of collisions easing the suspension of particles to higher positions in the tank.

Effect of solids concentration on cloud height at N_{js} were also investigated for Al_2O_3 and Garnet between 2 and 20 vol%. The results for these slurries are shown in Figure 4.11 in comparison with the MG slurry since the particle size of the three types of particles is very similar. This allows for an evaluation of the effect of solids concentration and density on cloud height simultaneously. At low solids concentrations, the difference between cloud height data of MG, Al_2O_3 and Garnet

are visible giving a maximum of 8%. At and above 6 vol%, cloud height data for all three particles overlap.

The trend of change of the cloud height with increasing solids concentration with Al_2O_3 and Garnet is similar to that of MG and other glass beads slurries shown in Figure 4.10. The slope of the initial sharp decrease between 2-7 vol% is less steep with Al_2O_3 and Garnet as given in Table 4.4. The data in Table 4.4 shows that the sharpness of the decrease in cloud height with increasing solids concentration significantly decreases as the density of the particle is increased.

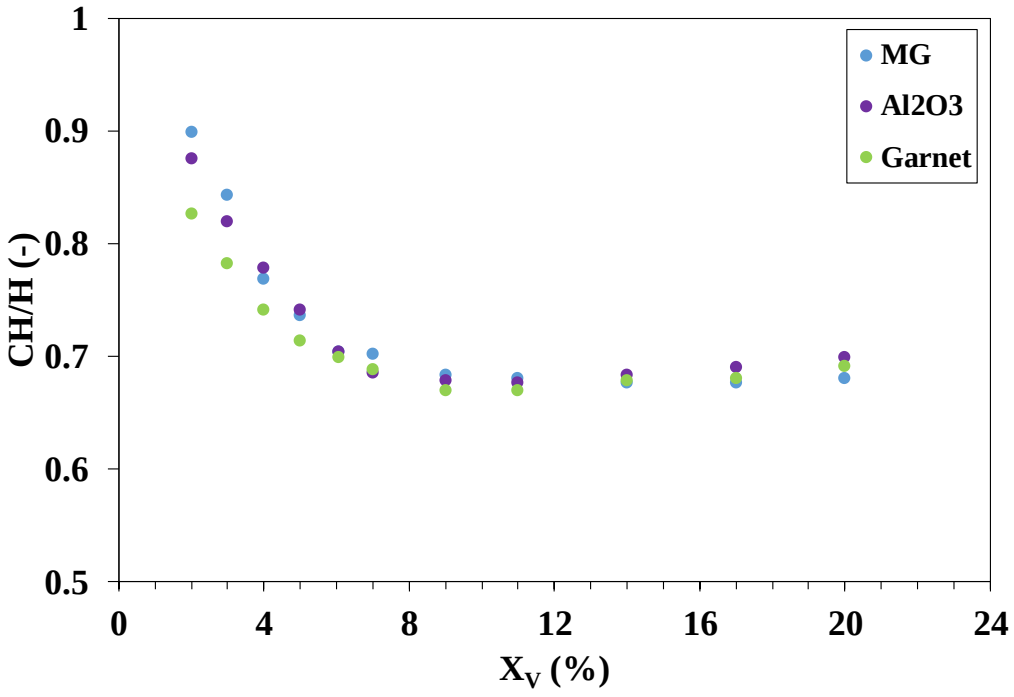

Figure 4.11. Variation of cloud height relative to the liquid height with increasing solids concentration for MG, Al_2O_3 and Garnet

Table 4.4 The exponents on X_V for particles that have similar densities between solids concentration of 2 and 7 vol%.

	Exponent of X_V
MG	-0.213
Al_2O_3	-0.198
Garnet	-0.155

4.2.2 Effect of Impeller Speed on Cloud Height

Impeller speed is one of the significant parameters that affect cloud height as mentioned before. The effect of impeller speed on cloud height was investigated to identify the limitations of impeller speed on the cloud height in Section 4.1.2.2. It was shown that cloud height changes non-monotonically as impeller speed was increased between 0.06-1.45 N/N_{js}. In this section, the effect of impeller speed on cloud height is at N/N_{js} of 0.8, 1, 1.2, 1.3 and 1.45, with the aim of correlating the cloud height and impeller speed. The N/N_{js} values were selected beginning from $N=0.8N_{js}$ since, generally lower impeller speeds are not preferred in most solid-liquid mixing applications. The upper limit of $N/N_{js}=1.45$ was determined based on the upper limit identified for observation of a meaningful cloud height in Section 4.1.2.2. The cloud height varies monotonically in the range of 0.8-1.45 N/N_{js}. SG, MG, LG, BG, Al_2O_3 and Garnet slurries at 5 vol% were tested.

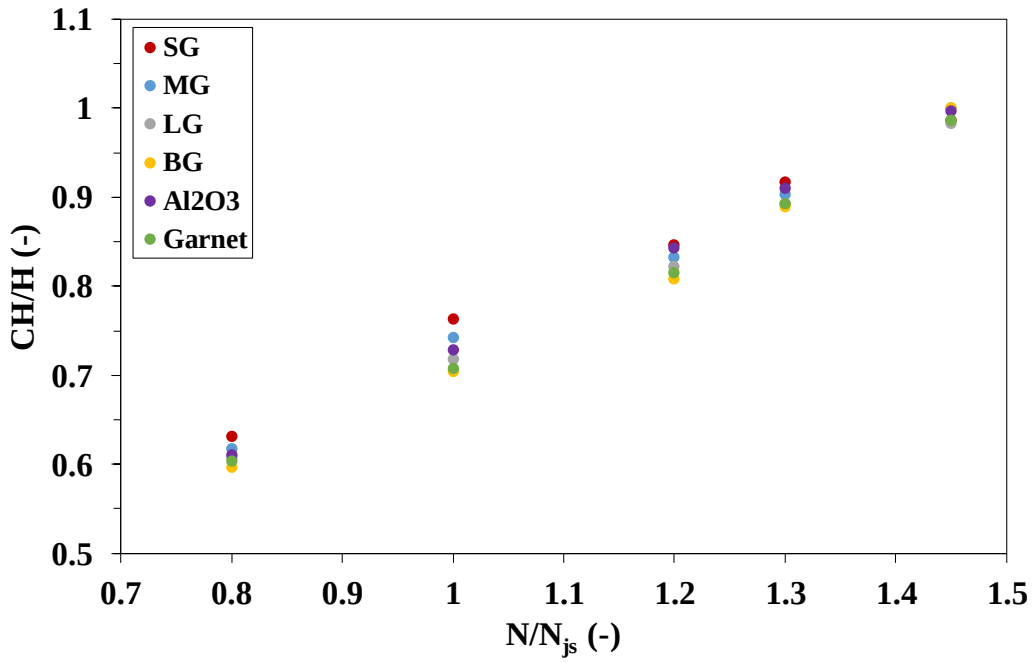

Figure 4.12. Variation of cloud height relative to the liquid height between 0.8-1.45 N/N_{js} for SG, MG, LG, BG, Al_2O_3 and Garnet slurries at 5 vol%.

Change in cloud height with increasing impeller speeds between $N=0.8N_{js}$ and $N=1.45N_{js}$ is given in Figure 4.12. Cloud height data of all particles increased with increasing impeller speed between 0.8-1.45 N/N_{js}. For all particles, increasing cloud height with increasing impeller speed are represented with the exponents given in Table 4.5.

Table 4.5 The exponents on N/N_{js} for SG, MG, LG, BG, Al_2O_3 and Garnet

	Exponent on N/N_{js}
SG	0.739
MG	0.790
LG	0.803
BG	0.853
Al_2O_3	0.823
Garnet	0.821

In Table 4.5 the particles are listed in the order of increasing particle size for the glass beads, and the sizes are similar for Al_2O_3, Garnet and MG. The exponents on N/N_{js} increase as the size of the particle is increased. However, for particles which have similar sizes but different densities – Al_2O_3, Garnet and MG – the exponents of N/N_{js} do not follow a trend. Increasing the particle density from MG to Al_2O_3 causes an increase in the exponent; however, almost no change is observed when the density is increased from Al_2O_3 to Garnet particles. Arithmetic mean of the exponents of all particles is 0.8. In the overall, this means that, cloud height was found to be proportional to $(N/N_{js})^{0.8}$ between 0.8-1.45 N/N_{js}.

An analysis on the power consumption is needed in order to bring all the solids to the liquid surface was performed. For all particles, the power consumption at $N=1.45Njs$ (P_{LH}) was compared with the power consumption at $N=N_{js}$ (P_{js}). The power consumption data is given in Table 4.6.

Table 4.6 Comparison of power consumption at $N=N_{js}$ and $N=1.45N_{js}$

	P_{js} (W)	P_{LH} (W)	P_{LH}/P_{js} (-)
SG	5.3	16.1	3.0
MG	9.5	29.9	3.1
LG	17.8	54.0	3.0
BG	19.2	64.3	3.3
Al_2O_3	29.0	90.0	3.1
Garnet	32.4	102.9	3.2

The power consumption at the degree of complete off-bottom suspension – at N_{js} – increases as the size and the density of the particle are increased. This is reasonable since just-suspended speed increases as the size and the density of the particle are increased. The power required to suspend solids up to the liquid surface is approximately three times the power required for complete off-bottom suspension condition. This means that in the operation, there is a significant increase in the

power demand when the solids are needed to be carried to the top of the tank. The design should be done carefully considering the power demand.

4.2.3 Effects of Particle Properties on Cloud Height

In this section, possible effects of the size and the density of the particle on cloud height will be discussed. The results of these investigations are given in following subsections in that order.

4.2.3.1 Effect of The Particle Size on Cloud Height

Analysis of the effects of particle diameter on cloud height was performed using 2 vol% slurries of SG, MG, LG and BG at N_{js}. In this analysis, the size of the particle was varied between 124 μm and 712 μm. Change in cloud height data with increasing particle size is given in Figure 4.13. Error bars in this figure show the percent variation between the three measurements.

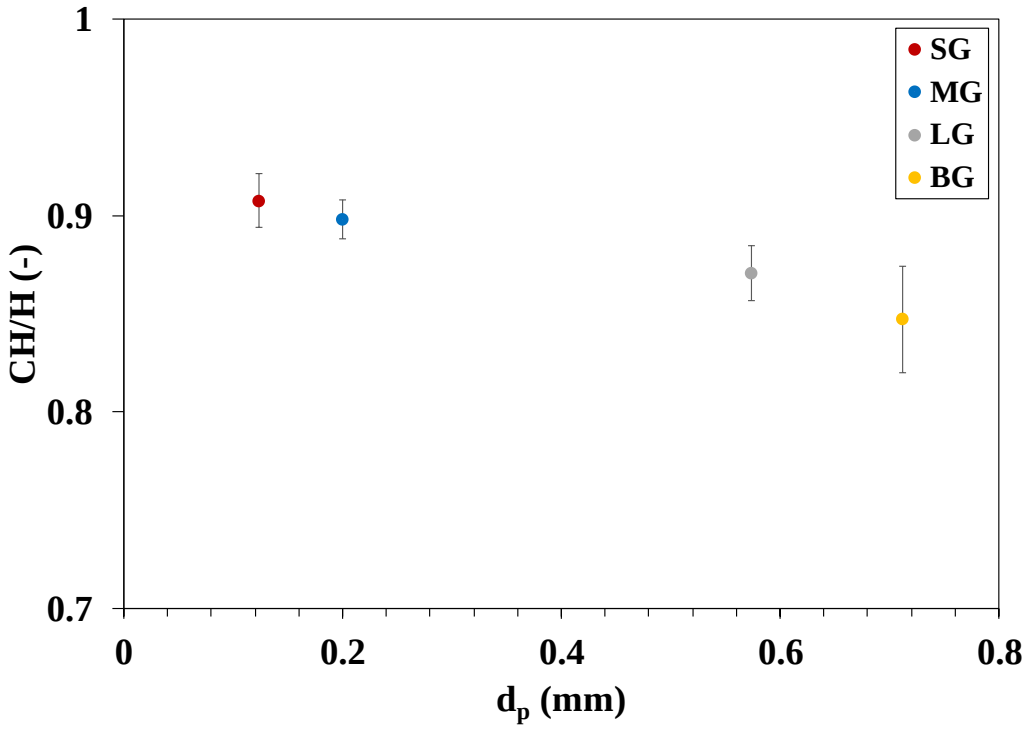

Figure 4.13. Variation of cloud height relative to the liquid height with an increase in size of the particle

As seen in Figure 4.13, a decrease in cloud height was observed as particle size was increased. This decrease in cloud height can be represented as an exponent of -0.036. It can be concluded that cloud height is not a strong function of particle diameter. A decreasing cloud height with increasing particle size was expected since a larger particle size means higher settling velocity and a particle with a higher settling velocity tends to settle more than a particle with a lower settling velocity.

In this analysis, one can consider that there are two competing parameters: the size of the particle and the number of the particles. In this study, the solids concentration values were determined dividing the volume of the solids by the total volume of the tank. The volume of the solids was equal to the mass of the solids divided by particle density. Thus, the weight of the solids which were loaded to the tank was the same for the particles with the same density, regardless of their sizes. However, at a fixed weight, the number of larger particles is less than the number of smaller particles.

Larger number of particles means a larger number of particle-particle collisions. The particle-particle collisions may not be dominant at relatively low solids concentrations, but they will play an important role as the solids concentrations are increased. In Figure 4.13, the smaller particles have larger cloud height. While the distribution of particles may be slightly affected by the larger number of particles and hence larger particle-particle collisions, it is not expected to play a significant role since the solids concentration is not sufficiently high to support such behavior.

During the experiments, it was also observed that the large particles formed a more compact cloud and a more clearly defined interface. One can expect that a more clearly pronounced solids cloud enables the cloud height measurements to be easier; however, the reality did not meet the expectation. This was due to the fluctuations in the interface increased as the size of the particle was increased. Similarly, Eng et al. (2015) observed larger temporal variations in cloud height of large particles, while they also observed the shape of the cloud to be more clearly pronounced in the experiments with large particles. Observing a more fluctuating interface with large particles may cause the variations between different measurements to increase. This might be the reason behind observing the largest error bar on the cloud height data of the largest particle in Figure 4.13.

4.2.3.2 Effect of The Density of The Particle on Cloud Height

The effects of the density of the particle on cloud height was investigated using 2 vol% slurries of MG, Al_2O_3, Garnet and Steel at N_{js}. In this analysis, the density of the particle was varied between 2500 kg/m^{3}and 7600 kg/m^3.

As seen in Figure 4.14, a decrease in cloud height was observed as the density of the particle was increased. This decrease in cloud height can be represented as an exponent of -0.123. It is concluded that cloud height is not a strong function of density of the particle. However, the density of the particle has a stronger effect on cloud height compared to the size of the particle.

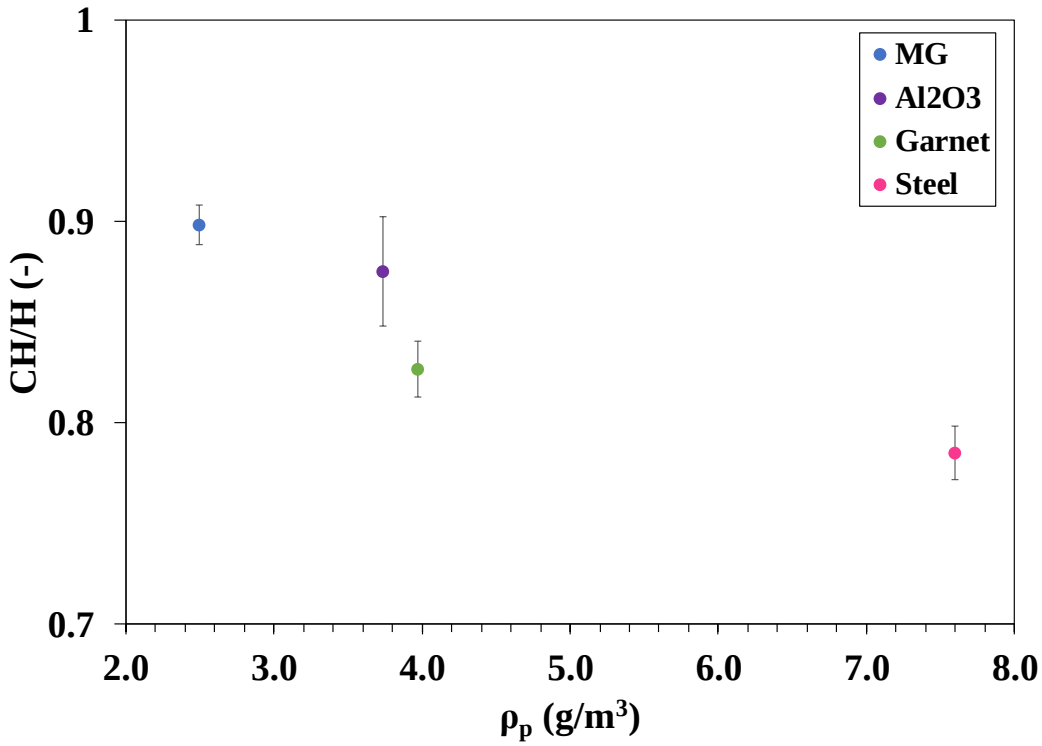

Figure 4.14. Variation of cloud height relative to the liquid height with an increase in density of the particle

Experiments performed for this analysis showed that density of the particle did not have a particular effect on fluctuations in the interface. The fluctuations observed in the experiments with SG –the smallest and lightest particle– were similar to the experiments with Steel – the most dense particle.

In Figure 4.14, the error bars show the variations between the three different measurements. The largest error percent is observed for Al_2O_3. This may not be related to the density of this particle. In the particle lot for Al_2O_3, there were some very small particles. These very small particles were suspended throughout the tank during the experiments, and they changed the color of the liquid-rich part to the color of Al_2O_3 particles. This made the cloud height measurements more challenging due

to poor color contrast at the level of cloud height. This may be the cause of the variation between different measurements to be the greatest for Al_2O_3. The particle size distribution of Al_2O_3 and the other particles are given in Appendix A.

4.2.4 Effects of Off-Bottom Clearance on Cloud Height

In this section, the results of the analysis on the effects of off-bottom clearance on cloud height is discussed. For this analysis, 5 vol% slurries of SG, MG, LG, BG, Al_2O_3 and Garnet was tested at N_{js}. Experiments were conducted at off-bottom clearances of 0.167, 0.25 and 0.33. For these experiments, N_{js} values were determined using the model that was proposed by Ayranci & Kresta (2014). The changes in the cloud height data of SG, MG, LG, and BG slurries with the increase in off-bottom clearance are given in Figure 4.15.

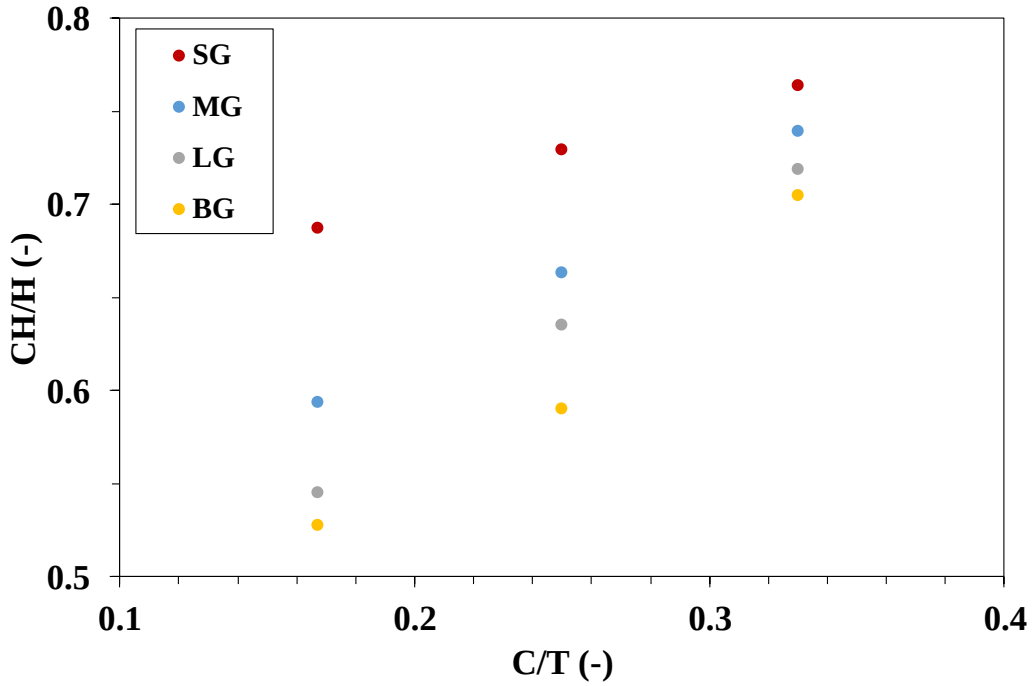

Figure 4.15. Variation of cloud height relative to the liquid height with increasing off-bottom clearance for SG, MG, LG and BG

As seen in Figure 4.15, for all particles, cloud height was observed to increase as off-bottom clearance was increased at N_{js}. As mentioned before, a system in which the impeller is placed in a lower position reaches the suspension degree of complete off-bottom suspension at a lower impeller speed compared to a system with a higher off-bottom clearance. Therefore, a system with a lower off-bottom clearance requires less energy to be operated at N_{js}. This energy may not be sufficient for the solids to reach the level that can be reached in a tank with higher off-bottom clearance. Thus, the higher the off-bottom clearance, the higher the cloud height at N_{js}, as seen in Figure 4.15.

The increase in cloud height with off-bottom clearance can be represented as exponents of 0.154, 0.319, 0.404 and 0.414 for SG, MG, LG and BG, respectively. This shows that the cloud height of larger particles tend to increase more rapidly than small particles as the off-bottom clearance is increased. The difference between cloud height values of the smallest and the largest particles is the greatest at the lowest off-bottom clearance while it is the smallest at the highest off-bottom clearance. The arithmetic mean of the exponents was found as 0.32.

The effects of off-bottom clearance on cloud height was also investigated using the particles that have similar sizes but different densities. In Figure 4.16, cloud height data of 5 vol% slurries of MG, Al_2O_3 and Garnet at three different C/T values of 0.167, 0.25 and 0.33 at N_{js} are shown.

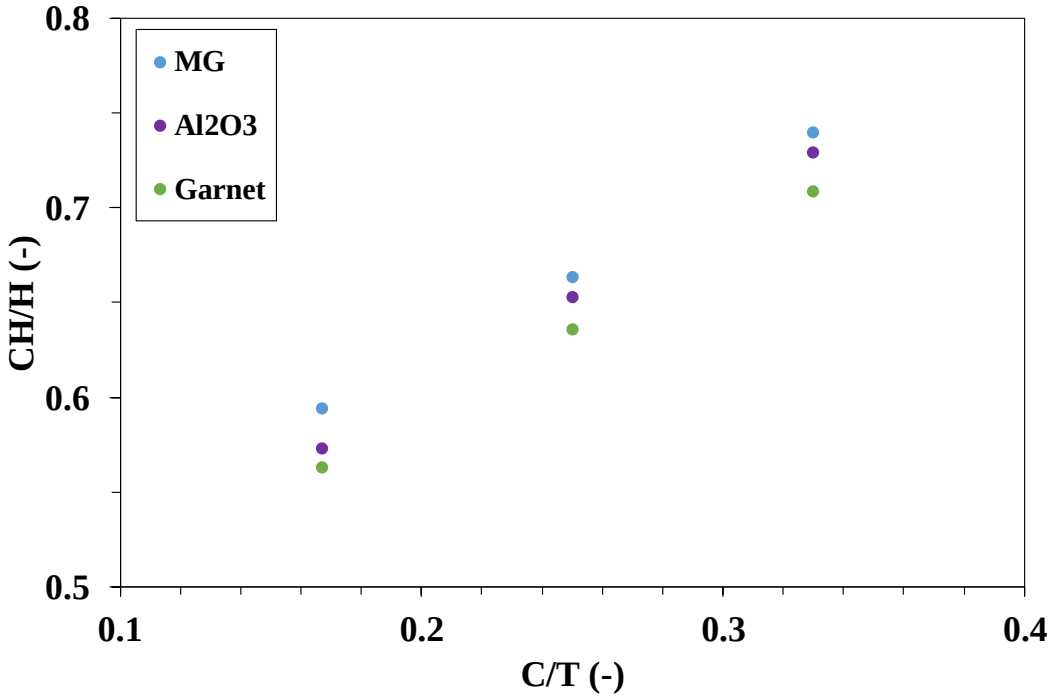

Figure 4.16. Variation of cloud height relative to the liquid height with increasing off-bottom clearance for MG, Al_2O_3 and Garnet

Similar to the previous analysis, for all particles, cloud height increases due to increasing off-bottom clearance as seen in Figure 4.16. This increase of cloud height can be represented as the exponents of 0.335 and 0.352 for Al_2O_3 and Garnet, respectively. Considering the exponent of 0.319 for MG, it was found that the exponent increased as the density of the particle was increased. Arithmetic mean of the exponents was found as 0.34 for MG, Al_2O_3 and Garnet. Considering all of the tests performed using six type of particles, the arithmetic mean of the exponent of C/T was calculated as 0.33. In other words, it was found that cloud height is proportional to $(C/T)^{0.33}$ at N_{js}.

The effect of the off-bottom clearance on cloud height was also investigated using 5 vol% slurries of LG, BG and Garnet at particular impeller speeds that were not related to N_{js} values of the corresponding particles. These slurries were tested at 500,

700, 800, 900, 1100 and 1300 rpm. The tests were performed at C/T values of 0.167, 0.25 and 0.33. For each particle N_{js} was different at each off-bottom clearance value. Thus, N/N_{js} value of the corresponding particle was different at each off-bottom clearance for one selected particular impeller speed. Let us take the slurry of Garnet into consideration to be tested at 700 rpm. At this impeller speed, N/ N_{js} value of this slurry changes between $N=0.6N_{js}$ and $N=0.78N_{js}$ at decreasing off-bottom clearances.

The results of this analysis are shown in Appendix B. The results showed that the change in cloud height with increasing off-bottom clearance was different for different ranges of N/N_{js}.

- Cloud height was observed to increase due to increasing off-bottom clearance between impeller speeds of $N=0.5N_{js}$ and $N=0.78N_{js}$.
- Cloud height was observed to behave non-monotonically due to increasing off-bottom clearance between impeller speeds of $N=0.7N_{js}$ and $N=N_{js}$. Cloud height first decreased then increased as off-bottom clearance was increased within this impeller speed range.
- Cloud height was observed to decrease due to increasing off-bottom clearance between impeller speeds of $N=0.93N_{js}$ and $N=1.78N_{js}$.

Further investigation may be required within an extensive range of N/N_{js} and a more comprehensive range of particle types to understand the effect of off-bottom clearance on cloud height.

All analysis presented in Section 4.2 was performed at N_{js}; that is, all experiments were performed at a different impeller speed since the N_{js} of each case were different. This might be considered as a competing parameter with the parameter that was under question. For instance, in Section 4.2.1, cloud height was investigated at increasing solids concentration; however, impeller speed at each solids concentration was also different. Solid-liquid mixing processes have quite complex nature; therefore, there might always be a competing parameter when the effect of a

particular parameter is investigated. Keeping the impeller speed constant at a selected value means the degree of suspension is not the same for all cases under investigation. It was believed that not being at the same degree of suspension would cause the analysis performed in this study to be questionable and unreliable; therefore, all analysis was performed at N_{js} due to being the key design parameter for solids suspensions. This provided all slurries to be at the same degree of suspension.

4.3 A Model That Predicts Cloud Height as A Function of Solids Concentration, Particle Properties and Off-Bottom Clearance

As mentioned in Chapter 2, in literature, there is only one model that predicts cloud height (Bittorf & Kresta, 2003). This model is a function of impeller speed and tank geometry. It does not involve parameters that represent solids concentration and particle properties, which were proven to affect cloud height in Section 4.2. At constant impeller speed and geometrical features of the tank, i.e. off-bottom clearance and impeller diameter, this model gives the same cloud height value regardless of the particle properties and concentration. The authors stated that this model is in good agreement with experimental data between CH/H 0.6 and 0.8 for an H=T tank. According to the findings presented in Section 4.1.1.1, in such a tank cloud height data between 0.6 and 0.8 CH/H can only result:

- at impeller speeds lower than N_{js} if $0.25 \leq C/T \leq 0.33$
- if $C/T<0.25$

It should be reminded that conducting a solids suspension process at impeller speeds lower than N_{js} is not reasonable in terms of efficiency for most industrial applications. The findings of this study clearly show that there is an effect of solids concentration and properties on the cloud height. This presents a need for developing a correlation for predicting cloud height that includes these parameters.

In this section, a model that predicts the cloud height as a function of solids concentration, particle properties and off-bottom clearance is proposed. Until this section all experiments, except for off-bottom clearance analysis, were performed in Setup 1. Due to the limitations of the experimental setup, experiments for off-bottom clearance could only be performed in Setup 2. With the aim of obtaining all the data that will be used for developing the correlation from the same setup, new data was collected for particle size, density and impeller speed parameters in Setup 2. This new data is at 5 vol%, whereas the previous data is at 2 vol%. The data for solids concentration was collected again in Setup 2, using slightly larger increments between data points. One significant difference between the data collected in the two setups is related to the N_{js}. N_{js} cannot be measured in Setup 2; therefore, it was determined using the model proposed by Ayranci & Kresta (2014). The difference for the data repeated between the two setups is maximum 7.9% which is most likely caused from the differences in the calculated versus measured N_{js} values. Since the data are very close and the trends are very similar for the repeated data and the new data presented in this section, the investigation focuses only on the development of the correlation. The data collected in the previous sections are used for testing the developed correlation. The data shown in this section is taken at a fixed C/T of 0.33 and impeller speed of $N=N_{js}$ if these two parameters are not the ones being investigated.

Figure 4.17 shows the data for all the particles tested in this study at solids concentration varying between 2 to 17 vol%. A power law fit was applied to the data sets for each particle over the entire solids concentration range. The fits are shown in the figure with dashed lines and the relevant equations are given next to the legend with the corresponding colour scheme for each particle. The arithmetic mean of the exponents that represent the decreasing trend of CH/H with increasing solids concentrations was calculated as -0.125.

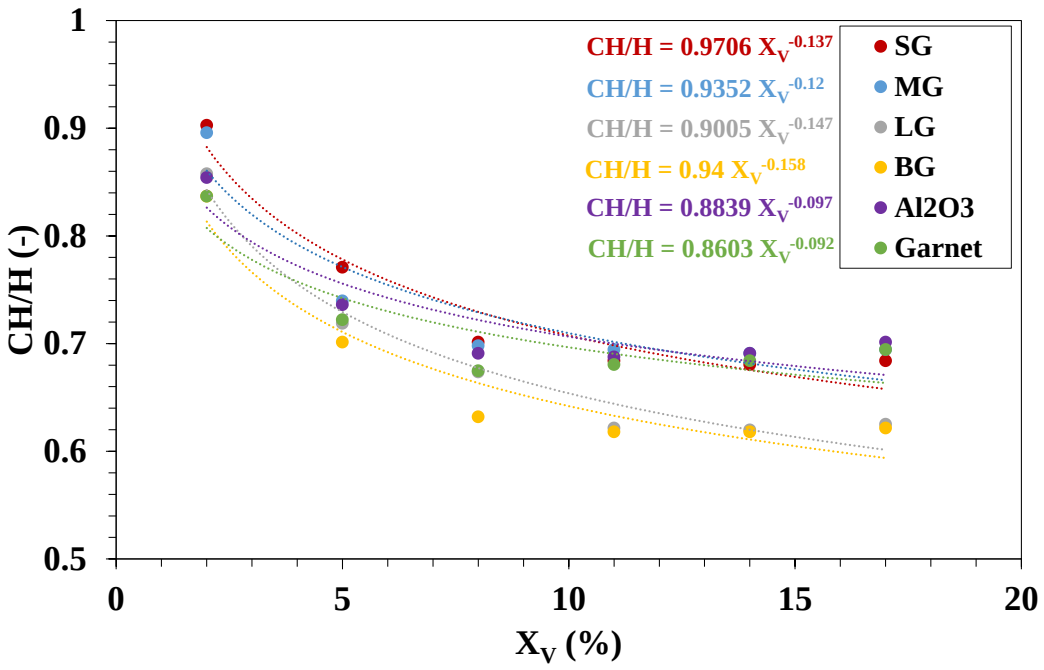

Figure 4.17. Variation of cloud height relative to the liquid height with increasing solids concentration

The experiments on the effect of density of the particle on cloud height was performed using slurries of MG, Al_2O_3, Garnet and Steel. Figure 4.18 shows the change in cloud height with increasing particle density. In x-axis of this figure, the density of the particle is given as $\Delta\rho/\rho_l$ since the density of the particle is represented as a dimensionless parameter in the model. Dimensionless density is varied between 1.5 and 6.6. The decrease in cloud height can be expressed with an exponent of -0.043. That is, cloud height was found to be proportional to $(\Delta\rho/\rho_l)^{-0.043}$. The value of R^2 is equal to 0.86.

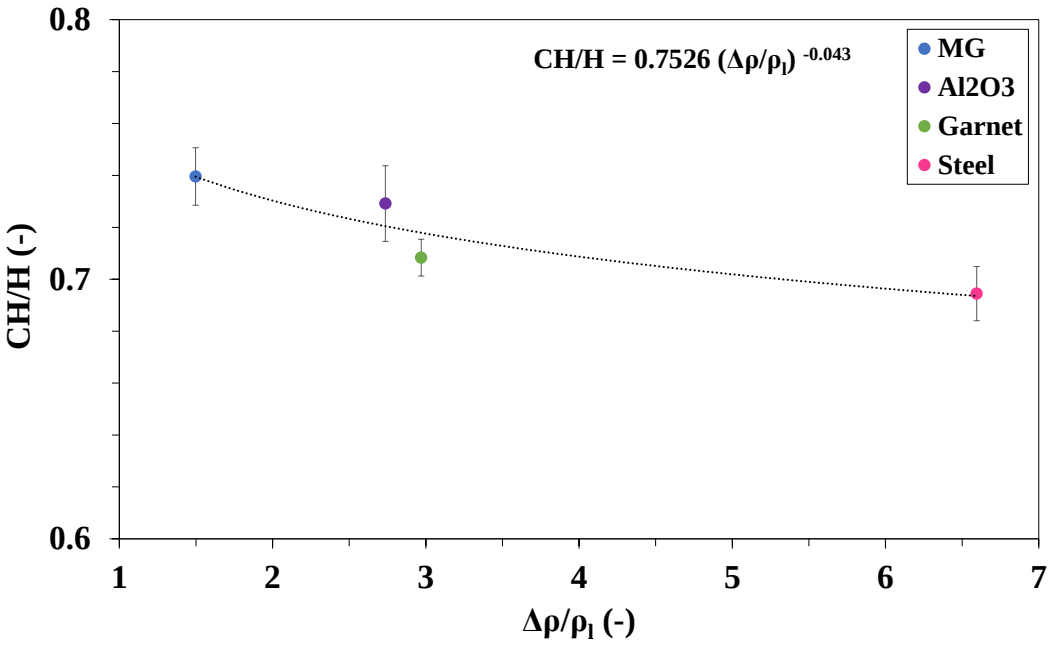

Figure 4.18. Variation of cloud height relative to the liquid height with an increase in density of the particle

The experiments on the effect of the size of the particle on cloud height was performed using slurries of SG, MG, LG and BG. The change in cloud height with increasing dimensionless particle size d_p/T is shown in Figure 4.19. Dimensionless particle size parameter is varied between 0.0015 and 0.0089. The decrease in cloud height can be expressed with an exponent of -0.041. That is cloud height was found to be proportional to $(d_p/T)^{-0.041}$. The value of R^2 is equal to 0.96.

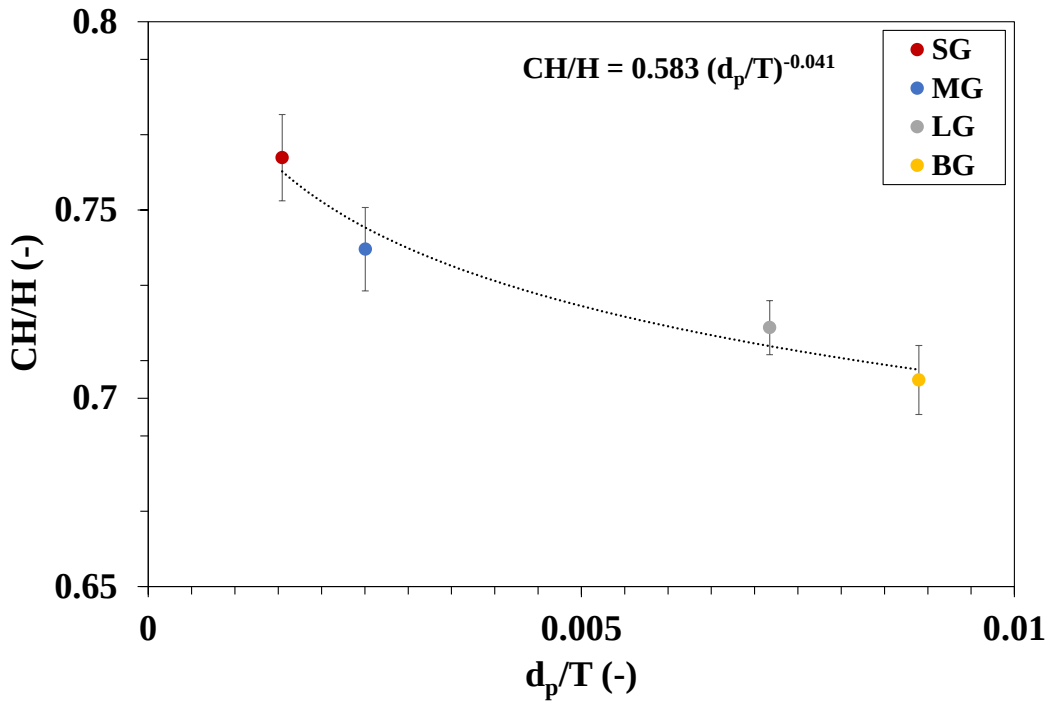

Figure 4.19. Variation of cloud height relative to the liquid height with an increase in size of the particle

Figure 4.20 shows the data given in Figure 4.15 and Figure 4.16 gathered together. The fits are shown in the figure with dotted lines and the relevant equations are given next to the legend with the corresponding colour scheme for each particle. The increase in cloud height for all particles can be expressed with an exponent of 0.33. This is the arithmetic mean of the exponents of power law functions which were fitted to cloud height data of all particles.

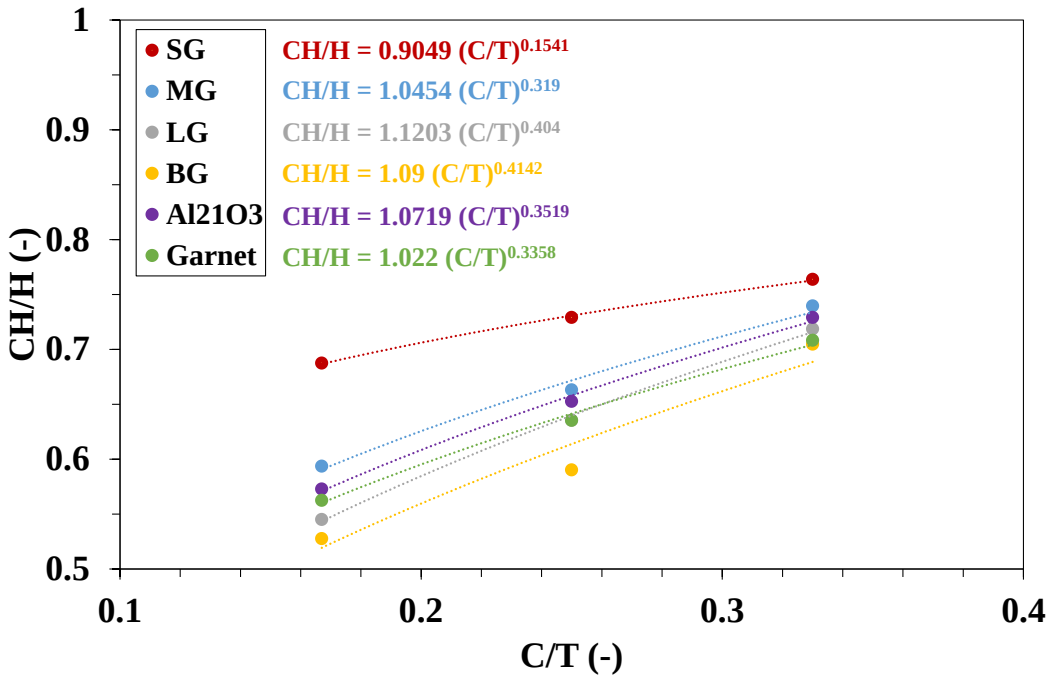

Figure 4.20. Variation of cloud height relative to the liquid height with increasing off-bottom clearance

The model that predicts cloud height as a function of solids concentration, physical properties of the particle and off-bottom clearance is developed in the form of the multiplication of the power law functions of all parameters. It should be reminded that the model is for the condition of complete off-bottom suspension, which means that the impeller speed is at N_{js} of each slurry. Using the exponents found from the analysis of all the parameters from Figures 17 to 20 the following model is found:

$$\frac{CH}{H} = (X_V)^{-0.125} \left(\frac{d_p}{T}\right)^{-0.041} \left(\frac{\Delta\rho}{\rho_l}\right)^{-0.043} \left(\frac{C}{T}\right)^{0.33} \quad (6)$$

Figure 4.21 shows the parity plot for this model. The dashed lines in this figure indicate ±20% error. While some of the data falls on the parity line, some of the data is underpredicted; however, all the data falls within the ±20% error lines.

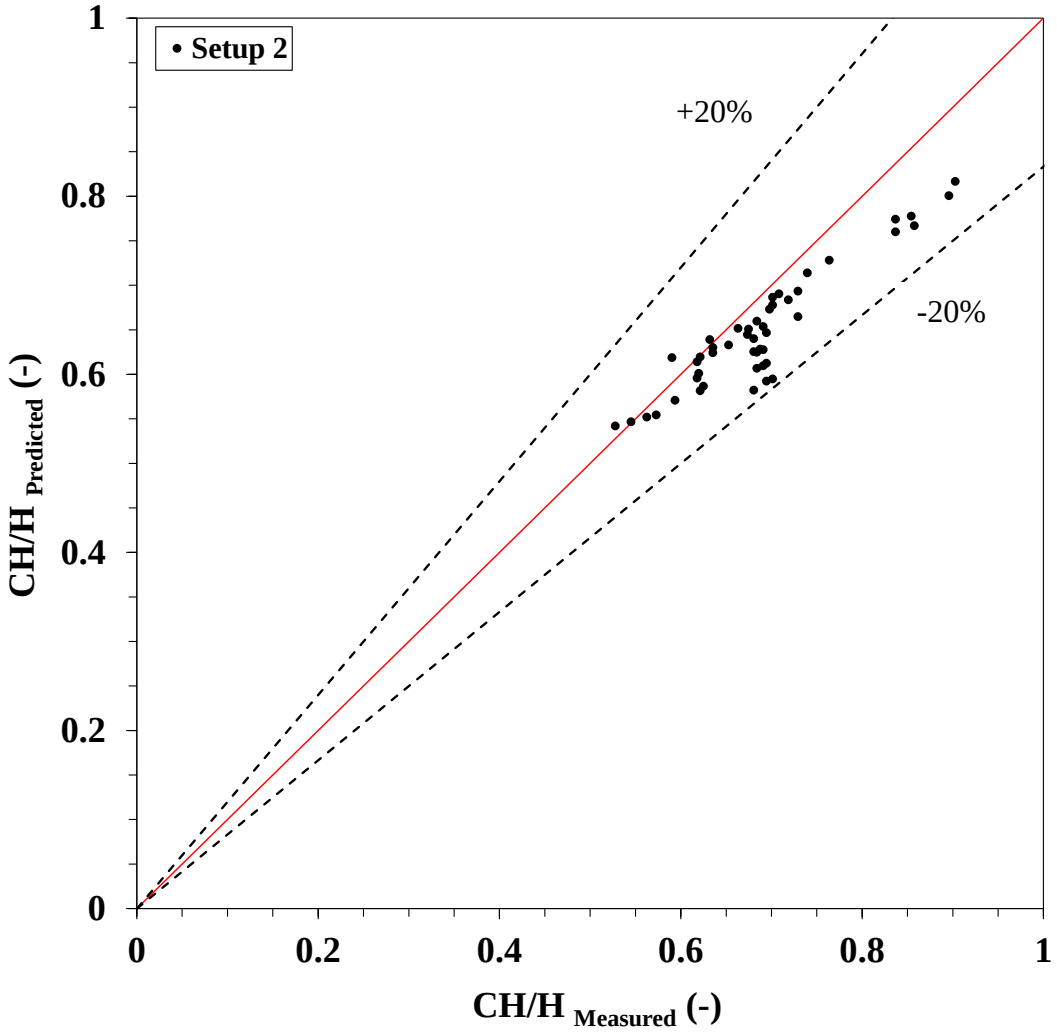

Figure 4.21. Comparison of the experimental cloud height relative to the liquid height and cloud height relative to the liquid height estimated from the correlation for data in Setup 2

Figure 4.22 shows the data that was obtained in Sections 4.2.1, 4.2.2, 4.2.3 and 4.2.4 in Setup 1, at a solids concentration of 2 vol% on top of the data given in Figure 4.21. This data set is shown with blue. The model predicts this data set also quite successfully as all fit in the ±20% error lines. This figure shows data also for a limited number of experiments conducted with thermoplastic elastomer (TPE) which has a density of 1165 kg/m^3 and a size of 3 mm. This data set is shown with yellow. The experiments with TPE were performed at two different off-bottom clearances and at 2 and 5 vol% solids concentrations. This particle was chosen for testing the limits of the model since the physical properties of TPE is quite different from the particles used in this study. The model is successful in predicting the cloud height for this particle, too. The standard deviation of cloud height data of TPE is calculated as 10.5%. Considering all the data in Figure 4.22, the standard deviation is calculated as 7.1%. Figure 4.22 involves 114 cloud height data. All data falls within the range of ±20%, which shows that the model is capable of predicting the cloud height successfully.

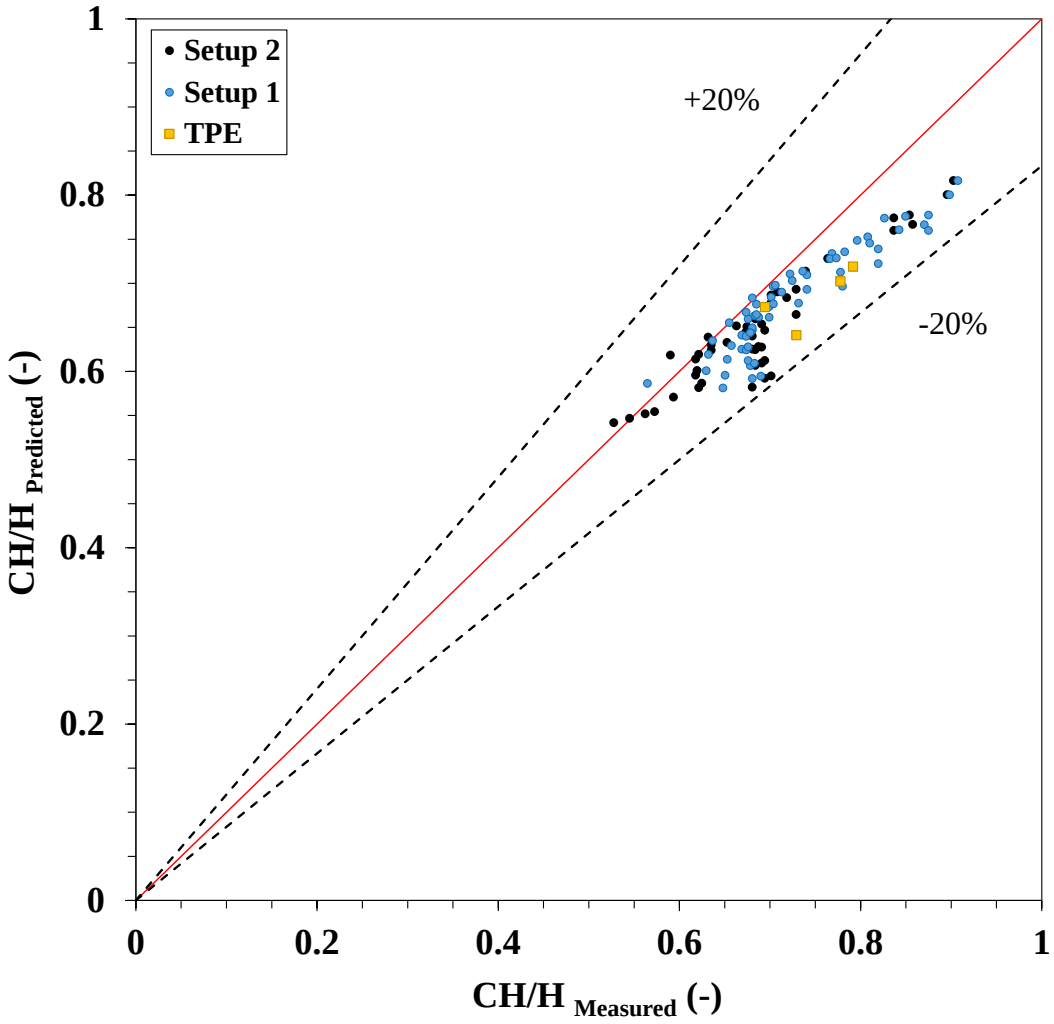

Figure 4.22. Comparison of the experimental cloud height relative to the liquid height and cloud height relative to the liquid height estimated from the correlation for data in both Setup 2 and Setup 1 and TPE data

As mentioned above, the model is for the condition of complete off-bottom suspension; however, investigations presented in Sections 4.1.2.2 and 4.2.2 showed that impeller speed is also an important parameter for cloud height. In Section 4.2.2, it was found that cloud height is proportional to $(N/N_{js})^{0.8}$ between 0.8-1.45 N/N_{js}. The model was modified to include this relation as the following:

$$\frac{CH}{H} = \left(\frac{N}{N_{js}}\right)^{0.8} (X_V)^{-0.125} \left(\frac{d_p}{T}\right)^{-0.041} \left(\frac{\Delta\rho}{\rho_l}\right)^{-0.043} \left(\frac{C}{T}\right)^{0.33} \quad (7)$$

The data obtained from the modified model is shown in green in Figure 4.23. The data set shown in Figure 4.22 was obtained at $N/N_{js}=1$; thus, it was not affected by the $(N/N_{js})^{0.8}$ term. This model predicts cloud height at varying impeller speeds with a standard deviation of 4.6%. The results of the modified model are promising. This model may be extended by further investigations on solids concentration, particle properties, and off-bottom clearance at different N/N_{js}.

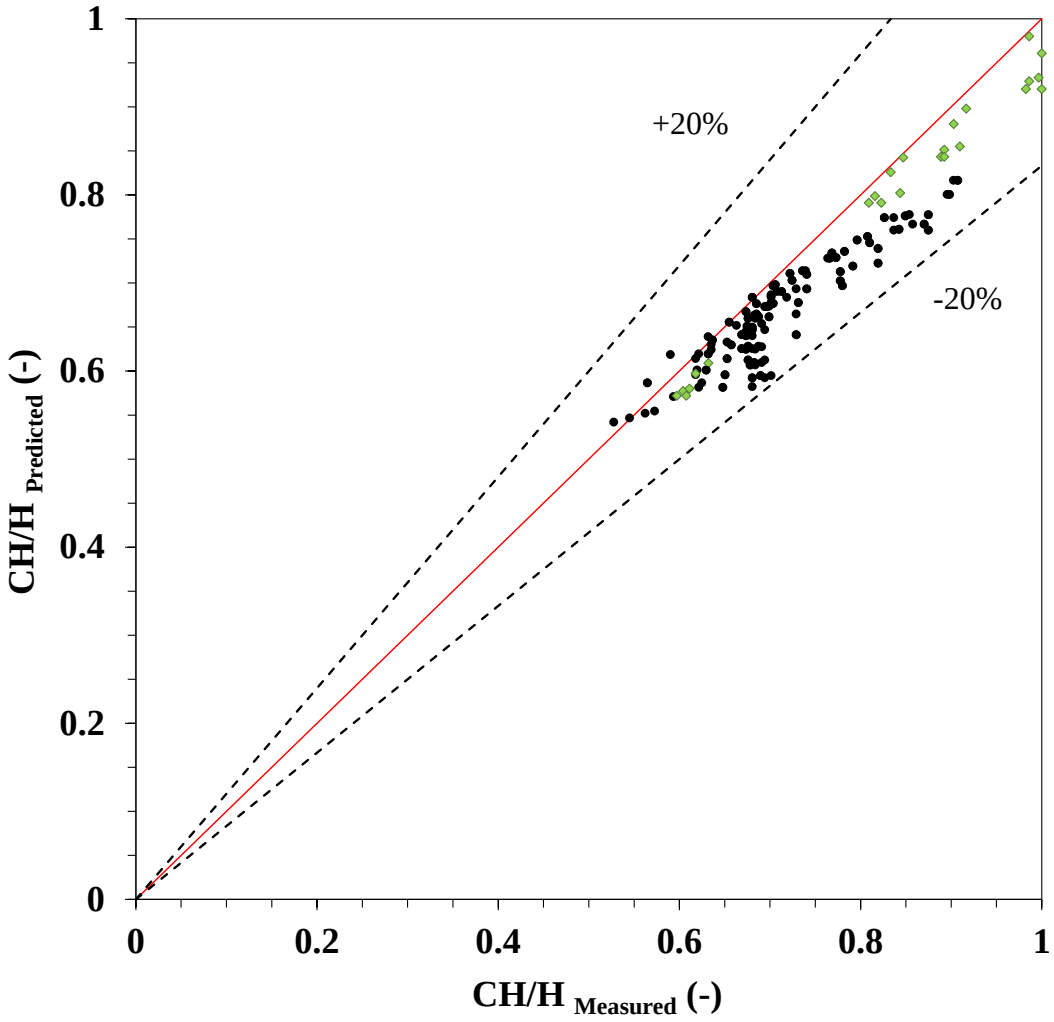

Figure 4.23. Comparison of the experimental cloud height relative to the liquid height and cloud height relative to the liquid height estimated from the correlation for both original and modified models. The data shown in green was obtained for cases where N is varied. The black data is the same as data given in Figure 4.22.

CHAPTER 5

CONCLUSIONS AND FUTURE WORK

5.1 Conclusions

Solids suspensions at high solids concentrations are extensively involved throughout most industrial solid-liquid mixing processes. Investigating the solids distribution in such solids suspension processes provides information about the efficiency of the process. Cloud height is the key design parameter for solids distribution. While there is no clear and comprehensive definition of cloud height in literature, in general terms cloud height is known as the height of the interface that forms at high solids concentrations. This study aims to clarify the current definition of cloud height to be detailed and applicable, and to investigate the effects of solids concentration and particle properties on cloud height, and to propose a model that predicts cloud height as a function of solids concentration, particle properties and off-bottom clearance. A measurement point of cloud height was determined, and the limitations and effects of solids concentration and impeller speed were identified in order to clarify the current definition of cloud height. Based on the clarified definition, the effects of solids concentration, particle properties and off-bottom clearance on cloud height was investigated. In the light of the findings, a model that predicts cloud height as a function of solids concentration, particle properties and off-bottom clearance was proposed.

In this thesis the following outcomes were found:

- Cloud height should be measured at the maximum point that solid particles can reach in the existence of a distinct interface. The rare, intermittent bursts of only a few solid particles should be excluded.

- Solids occupy all the tank volume in tanks with H=T operating at N_{js} at solids concentrations varying between 9 – 25 vol% when off-bottom clearance is set at the position that is equal to T/3 and T/4. There is no cloud height under these conditions since an interface does not form.

- It is recommended to use volume percent in identifying the relation between cloud height and solids concentration as it provides the same limits among different particle types.

- At low solids concentrations, at N_{js}, there is no clear interface between solid-rich and liquid-rich parts of the vessel. The lower limit on solids concentration for a meaningful cloud height data is 2 vol%. Increasing the solids concentration causes a decrease in cloud height up to 9 vol%. Above 9 vol% cloud height is not affected significantly by the increase in solids concentration. This shows that reporting a cloud height is not meaningful below 2 vol%, and that a persistent cloud height appears above 9 vol%.

- At low impeller speeds, there is no clear interface between solid-rich and liquid-rich parts of the vessel. The lower limit on impeller speed for a meaningful cloud height data is $N=0.32N_{js}$. Cloud height shows non-monotonic behavior as impeller speed is increased. At very high impeller speeds, at and above $N=1.45N_{js}$, no interface is observed since solids cover all the tank volume. This means that a cloud height does not form above $N=1.45N_{js}$ for a system in which H=1.5T.

- A clear definition of cloud height that addresses the aforementioned limitations is the following:

  > Cloud height can be measured only when an interface forms between the solid-rich and liquid-rich volumes. The height of this interface should be measured at the maximum height that solids can reach, which is in front of the baffle. Cloud height occurs at and above an impeller speed of $N=0.32N_{js}$ and at and above a solids concentration

of 2 vol%. A persistent cloud height is achieved above 9 vol%. The cloud height disappears beginning from $N=1.45N_{js}$ for a tank with H=1.5T, as the solids cover the entire tank.

- Cloud height increases as the impeller speed is increased between 0.8-1.45 N/N_{js}. For SG, MG, LG, BG, Al_2O_3 and Garnet, cloud height reaches liquid surface at $N=1.45\ N/N_{js}$. For all particle types, power required to distribute solids throughout the tank is three times the power consumption at just-suspended condition.

- Cloud height is a strong function of solids concentration between 2 and 7 vol%. Increasing solids concentration within this range causes a decrease in cloud height at N_{js}. This decrease can be represented with an exponent of -0.213.

- Cloud height is not a strong function of particle size. Increasing particle size causes a slight decrease in cloud height at N_{js}. This decrease in cloud height can be represented with an exponent of -0.036 on d_p. Increasing the particle density causes a decrease in cloud height at N_{js}, which can be represented as an exponent of -0.123 on ρ_p.

- Cloud height is a strong function of the off-bottom clearance. Increasing the off-bottom clearance causes an increase in cloud height at N_{js}. This increase in cloud height can be represented with an exponent of 0.33. The off-bottom clearance affects cloud height differently in different ranges of N/N_{js}. Increasing the off-bottom clearance causes an increase between $N=0.5N_{js}$ and $N=0.78N_{js}$; first a decrease then an increase between $N=0.7N_{js}$ and $N=N_{js}$; and an increase in between $N=0.93N_{js}$ and $N=1.77N_{js}$.

- A purely empirical model that predicts cloud height as a function of solids concentration, particle properties and off-bottom clearance within an error of ±20% was proposed. This model predicts cloud height at just-suspended

condition at which maximum contact between two phases is provided at minimum power consumption. The model that proposed in this study is:

$$\frac{CH}{H} = (X_V)^{-0.125} \left(\frac{d_p}{T}\right)^{-0.041} \left(\frac{\Delta\rho}{\rho_l}\right)^{-0.043} \left(\frac{C}{T}\right)^{0.33}$$

5.2 Future Work

In this thesis, the current definition of cloud height was clarified by the determination of a measurement point and identification of limitations on solids concentration and impeller speed. The effects of solids concentration, particle properties and off-bottom clearance were investigated. Based on the findings, an empirical model that predicts cloud height as a function of solids concentration, particle properties and off-bottom clearance was proposed. Topics that can be investigated to improve this work and provide more knowledge about the parameters that affect cloud height are summarized as the following:

- The most effective impeller types for solids suspension are axial and mixed flow impellers. In this study, a 45º down-pumping PBT, which is a mixed flow impeller, was used as. This resulted in an inclined shape of cloud height across the cross-section of the tank. In case of using an axial impeller, an inclined cloud height might not form due to the flow pattern created by this impeller. While this may not have an effect on the measurement point of the cloud height since the solids will most likely be suspended to the same or similar points with this impeller, an investigation would be useful to extend or modify the proposed definition of the cloud height.
- Investigations on the off-bottom clearance showed that increasing the off-bottom clearance affects cloud height differently at different ranges of N/N_{js}. Cloud height increased, or decreased, or first decreased, then increased at increasing off-bottom clearance within different N/N_{js} ranges. The limits of these ranges of N/N_{js} were determined based on a limited number of

experiments. A further investigation with an extensive range of N/N_{js} is recommended.

- A model that predicts cloud height as a function of solids concentration, particle properties, and off-bottom clearance was proposed. This is the original form of the model, and it was developed for complete off-bottom suspension condition. In addition, the model was modified by including the effect of impeller speed on cloud height as a multiplier. The revised model gave successful cloud height predictions at varying impeller speeds. An extension on the investigation of the effect of impeller speed to cover a wider range of particle properties and impeller speeds could improve the model.

REFERENCES

Atiemo-Obeng, V. A., Penney, R. W., & Armenante, P. (2004). Solid-Liquid Mixing. In: Paul EL, Atiemo-Obeng VA, Kresta SM, Eds. Handbook of Industrial Mixing: Science and Practice. *John Wiley & Sons.*

Ayranci, I., & Kresta, S. M. (2014). Critical analysis of Zwietering correlation for solids suspension in stirred tanks. *Chemical Engineering Research and Design*, *92*(3), 413–422. https://doi.org/10.1016/j.cherd.2013.09.005

Ayranci, I., & Kresta, S. M. (2021). Turbulence damping above the cloud height in suspensions of concentrated slurries in stirred tanks. *AIChE Journal*, *January*, 2–10. https://doi.org/10.1002/aic.17207

Baldi, G., Conti, R., & Alaria, E. (1978). Complete suspension of particles in mechanically agitated vessels. *Chemical Engineering Science*, *33*(1), 21–25. https://doi.org/10.1016/0009-2509(78)85063-5

Bittorf, K. J., & Kresta, S. M. (2003). Prediction of cloud height for solid suspensions in stirred tanks. *Chemical Engineering Research and Design*, *81*(5), 568–577. https://doi.org/10.1205/026387603765444519

Brown, D. A. R. (2018). Effect of D/T, Po, X, Viscosity, Specific Power Input and Scale on Solids Cloud Height in Stirred Vessels. *North American Mixing Forum*.

Bujalski, W., Takenaka, K., Paolini, S., Jahoda, M., Paglianti, A., Takahashi, K., Nienow, A. W., & Etchells, A. W. (1999). Suspension and liquid homogenization in high solids concentration stirred chemical reactors. *Chemical Engineering Research and Design*, *77*(3), 241–247. https://doi.org/10.1205/026387699526151

Davies, J. T. (1986). Particle Suspension and Mass Transfer Raies in Agitated Vessels Suspension von Partikeln und Stomibergang. *Chem. Eng. Proc.*, *20*,

175–181.

Eng, M., Rasmus, J., & Rasmuson, A. (2015). Analysis of Particle Cloud Height Dynamics in a Stirred Tank. *AIChE Journal*, *62*(1), 338–348. https://doi.org/10.1002/aic

Hicks, M. T., Myers, K. J., & Bakker, A. (1997). Cloud height in solids suspension agitation. *Chemical Engineering Communications*, *160*, 137–155. https://doi.org/10.1080/00986449708936610

Hosseini, S., Patel, D., Ein-Mozaffari, F., & Mehrvar, M. (2010). Study of solid-liquid mixing in agitated tanks through computational fluid dynamics modeling. *Industrial and Engineering Chemistry Research*, *49*(9), 4426–4435. https://doi.org/10.1021/ie901130z

Jafari, R., Tanguy, P. A., & Chaouki, J. (2012). Experimental investigation on solid dispersion, power consumption and scale-up in moderate to dense solid-liquid suspensions. *Chemical Engineering Research and Design*, *90*(2), 201–212. https://doi.org/10.1016/j.cherd.2011.07.009

Kasat, G. R., Khopkar, A. R., Ranade, V. V., & Pandit, A. B. (2008). CFD simulation of liquid-phase mixing in solid-liquid stirred reactor. *Chemical Engineering Science*, *63*(15), 3877–3885. https://doi.org/10.1016/j.ces.2008.04.018

Kraume, M. (1992). Mixing times in stirred suspensions. *Chemical Engineering & Technology*, *15*(5), 313–318. https://doi.org/10.1002/ceat.270150505

Kresta, S. M., Etchells, A. W., Dickey, D. S., & Atiemo-Obeng, V. A. (2016). Cfd Modeling Of Stirred Tank Reactors. John Wiley & Sons, Inc.

Kutukcu, B., & Ayranci, I. (2019). Application of pressure gauge measurement method beyond its limits. *Chemical Engineering Research and Design*, *141*, 170–180. https://doi.org/10.1016/j.cherd.2018.10.032

Lassaigne, M., Blais, B., Fradette, L., & Bertrand, F. (2016). Experimental investigation of the mixing of viscous liquids and non-dilute concentrations of

particles in a stirred tank. *Chemical Engineering Research and Design*, *108*, 55–68. https://doi.org/10.1016/j.cherd.2016.01.005

Leng, D. E., & Calabrese, R. V. (2004). Immiscible Liquid–Liquid Systems. In: Paul EL, Atiemo-Obeng VA, Kresta SM, Eds. Handbook of Industrial Mixing: Science and Practice. *John Wiley & Sons.*

Matthias Eng, Rasmus Jonsson, and A. R. (2015). Analysis of Particle Cloud Height Dynamics in a Stirred Tank. *AIChE Journal*, *62*(1), 33348. https://doi.org/10.1002/aic.15051

Micale, G., Grisafi, F., Rizzuti, L., & Brucato, A. (2004). CFD simulation of particle suspension height in stirred vessels. *Chemical Engineering Research and Design*, *82*(9 SPEC. ISS.), 1204–1213. https://doi.org/10.1205/cerd.82.9.1204.44171

Middleton, J. C., & Smith, J. M. (2004). Gas–Liquid Mixing in Turbulent Systems. In: Paul EL, Atiemo-Obeng VA, Kresta SM, Eds. Handbook of Industrial Mixing: Science and Practice. *John Wiley & Sons*.

Musil, L. (1984). Expansion of fluidized solids' layer at the critical impeller speed marking the onset of a complete suspension. *Chemical Engineering Science*, *39*(4), 629–636. https://doi.org/10.1016/0009-2509(84)80169-4

Ochieng, A., & Lewis, A. E. (2006). CFD simulation of solids off-bottom suspension and cloud height. *Hydrometallurgy*, *82*(1–2), 1–12. https://doi.org/10.1016/j.hydromet.2005.11.004

Sardeshpande, M. V., Juvekar, V. A., & Ranade, V. V. (2010). Hysteresis in Cloud Heights During Solid Suspension in Stirred Tank Reactor: Experiments and CFD Simulations. *AIChE Journal*, *56*(11), 2795–2804.

Sardeshpande, M. V., Sagi, A. R., Juvekar, V. A., & Ranade, V. V. (2009). Solid suspension and liquid phase mixing in solid-liquid stirred tanks. *Industrial and Engineering Chemistry Research*, *48*(21), 9713–9722.

https://doi.org/10.1021/ie801858a

Špidla, M., Sinevič, V., Jahoda, M., & MacHoň, V. (2005). Solid particle distribution of moderately concentrated suspensions in a pilot plant stirred vessel. *Chemical Engineering Journal*, *113*(1), 73–82. https://doi.org/10.1016/j.cej.2005.08.005

Xu, Z., Jin, Z., Liu, B., & Bengt, S. (2019). Experimental investigation on solid suspension performance of coaxial mixer in viscous and high solid loading systems. *Chemical Engineering Science*, *208*, 115144. https://doi.org/10.1016/j.ces.2019.08.002

Zhao, H. L., Zhang, Z. M., Zhang, T. A., Liu, Y., Gu, S. Q., & Zhang, C. (2014). Experimental and CFD studies of solid-liquid slurry tank stirred with an improved Intermig impeller. *Oral Oncology*, *50*(10), 2650–2659. https://doi.org/10.1016/S1003-6326(14)63395-1

Zwietering, T. . (1958). Suspending of solid particles in liquid by agitators. *Chemical Engineering Science*, *8*, 244–253.

APPENDICES

A. Particles Size Distribution

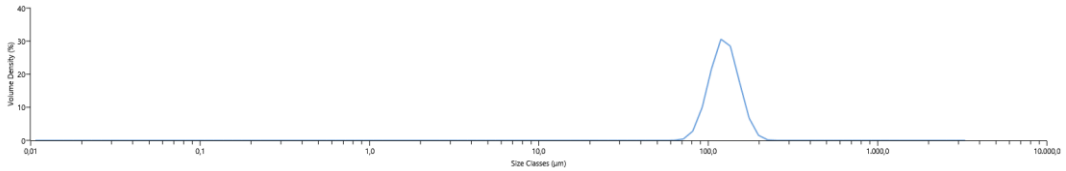

Figure A.1. Particle size distribution of SG

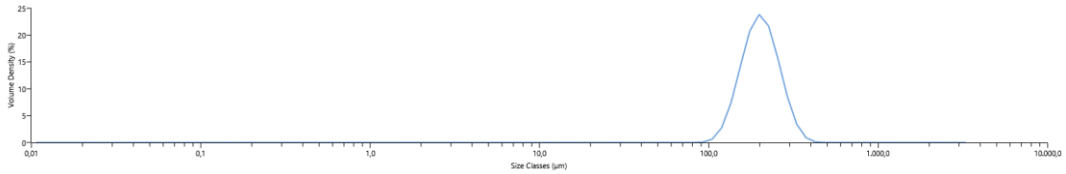

Figure A.2. Particle size distribution of MG

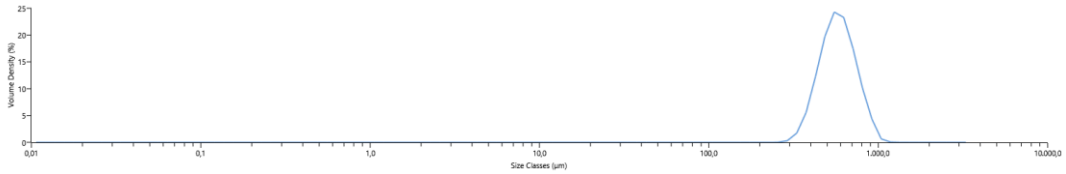

Figure A.3. Particle size distribution of LG

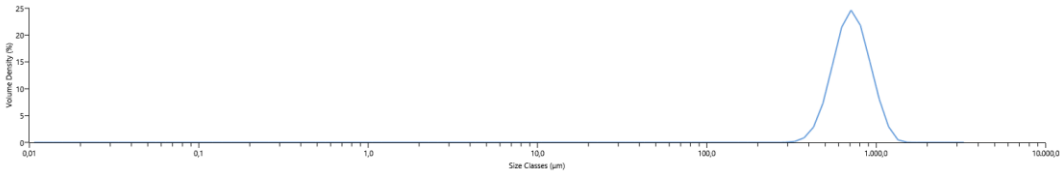

Figure A.4. Particle size distribution of BG

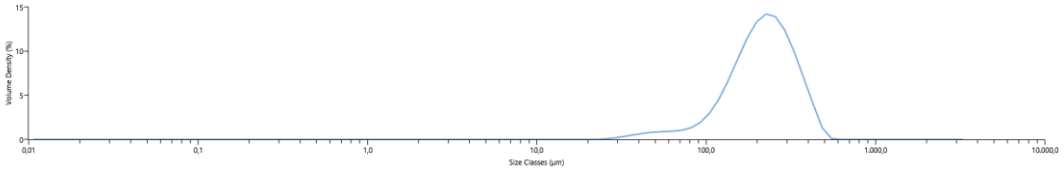

Figure A.5. Particle size distribution of Al_2O_3

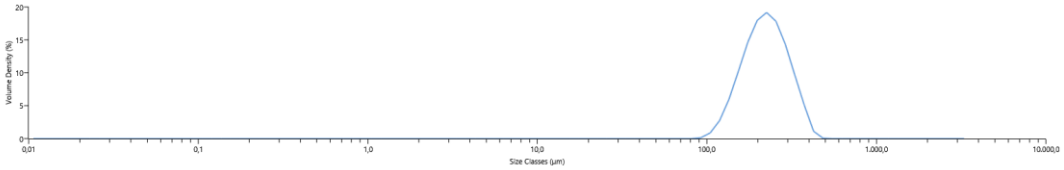

Figure A.6. Particle size distribution of Garnet

B. Effect of Off-Bottom Clearance on Cloud Height at Different Ranges of N/N_{js}

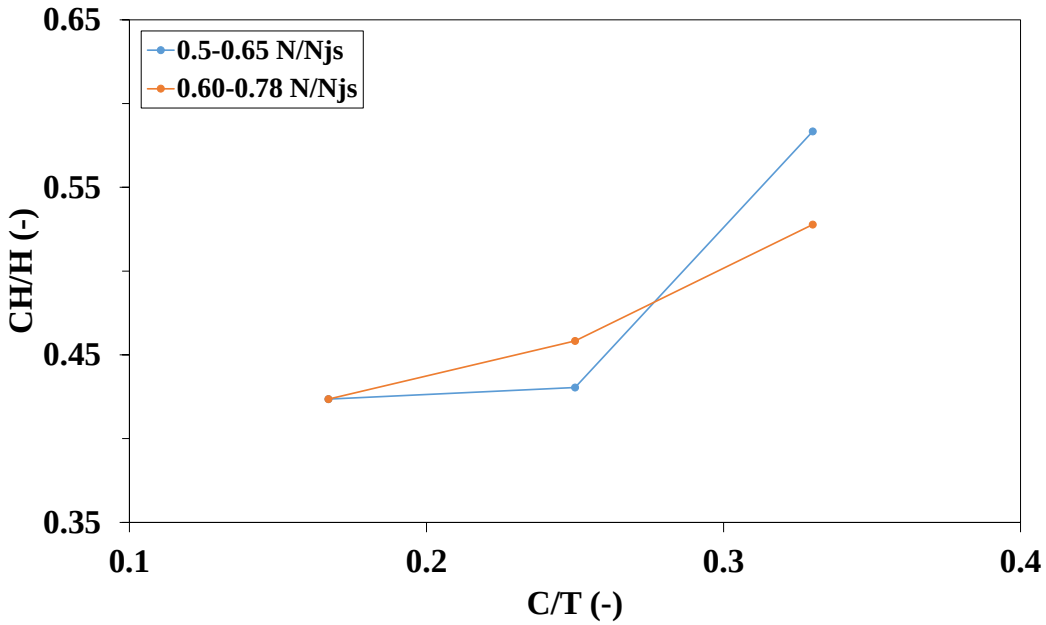

Figure B.7. Variation of cloud height relative to the liquid height with increasing off-bottom clearance between 0.5-0.78 N/N_{js}

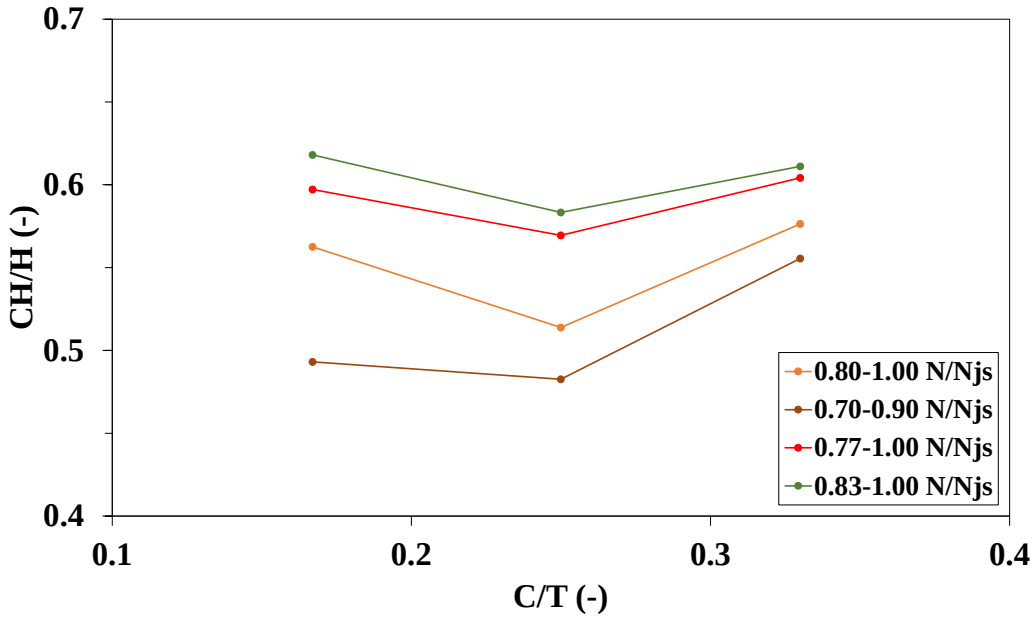

Figure B.8. Variation of cloud height relative to the liquid height with increasing off-bottom clearance between 0.7-1 N/N_{js}

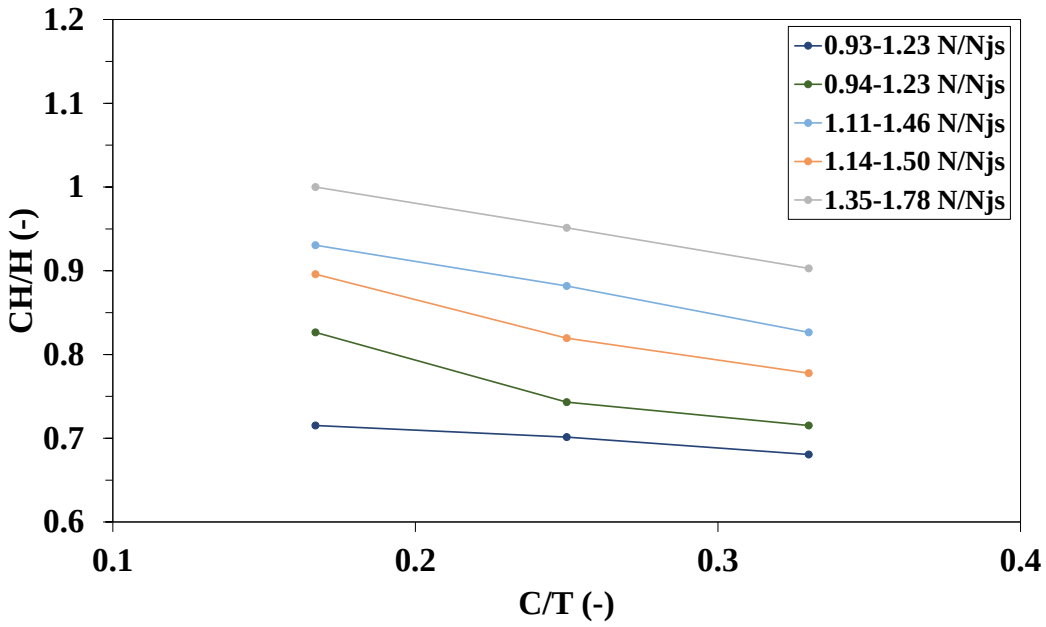

Figure B.9. Variation of cloud height relative to the liquid height with increasing off-bottom clearance between 0.93-1.78 N/N_{js}